Neutron Spectrometry and Dosimetry at high latitudes CORA Project

A.Zanini INFN Torino

CORA Project

(**CO**smic **R**ays in **A**ntarctic)

Ionizing radiation measurements campaign at Marambio Base -*Istituto Antartico Argentino*

Università di La Plata, Argentina

INFN Sez. Torino, Italy

Ecole Internationale Daniel Chalonge, France

Università di Torino, Italy

Marambio Base

(64 13’S – 56 43’W)

GV 0.22

Belgrano Base

(77°52′ S- 34°37′ W)

GV 0.86

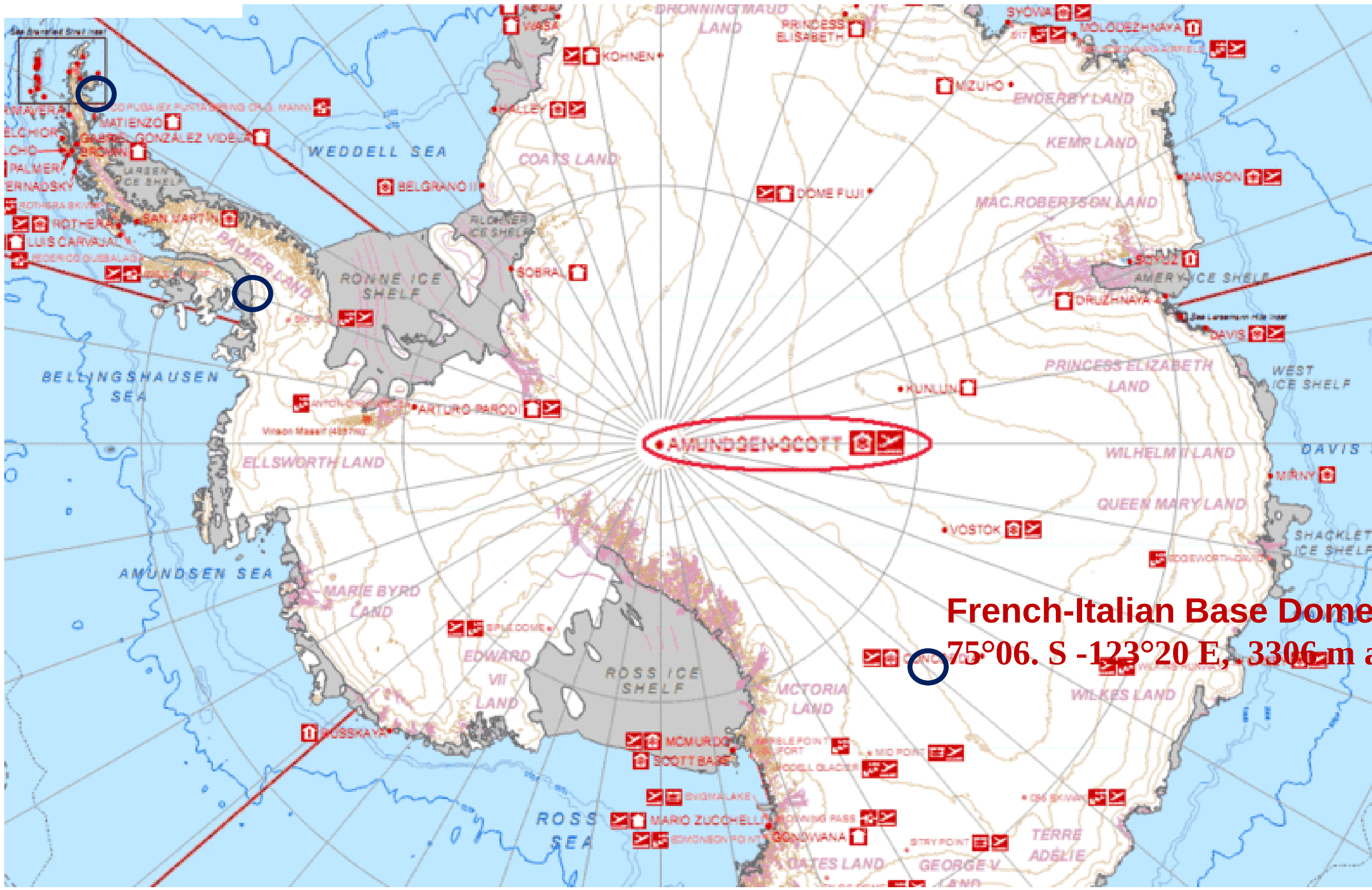

French-Italian Base Dome C

75°06. S -123°20 E, 3306 m asl.

Cosmic radiation

- The radiation environment around the Earth arises as a result of the interaction of primary galactic cosmic rays (GCR) with nuclei constituting the atmosphere.

- Primary particles, (87% protons, 11% alpha particles, 2% Heavy Nuclei) entering into the upper layers of the atmosphere, mainly interact with Oxigen (21%) and Nitrogen(78 %) nuclei and produce a secondary shower, consisting of different particles as protons, neutrons and mesons which can penetrate deeper into the atmosphere, undergoing further collisions, that leads to a cascade of particles.

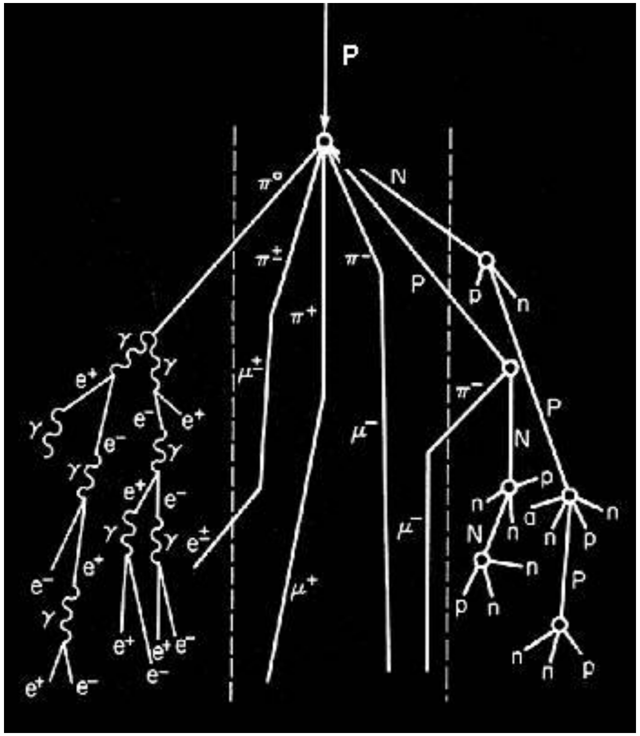

Atmospheric shower due to interaction of primary proton with O^{16} nucleus

Primary Cosmic rays composition

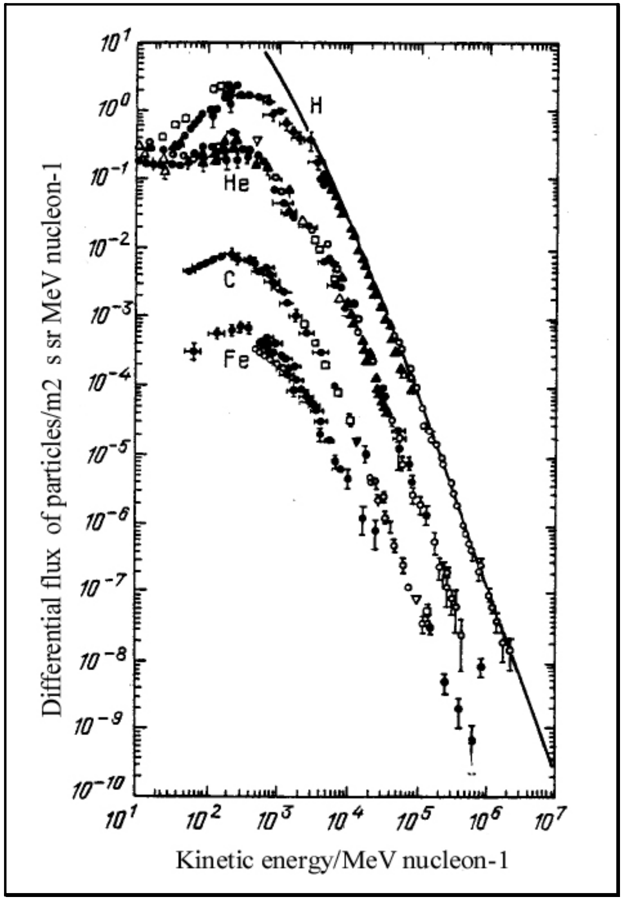

Energy spectrum of various components of primary cosmic rays

Cosmic Rays variability on Earth

The radiation environment and consequently the human being exposure, varies
1 –with altitude-because of the reduced thickness of atmosphere layer-
2- with latitude-because of the shape of the earth magnetic field-
3- with solar activity- because of the influence of solar wind on the galactic and extragalactic cosmic rays fluence, following a 11 years cycle.

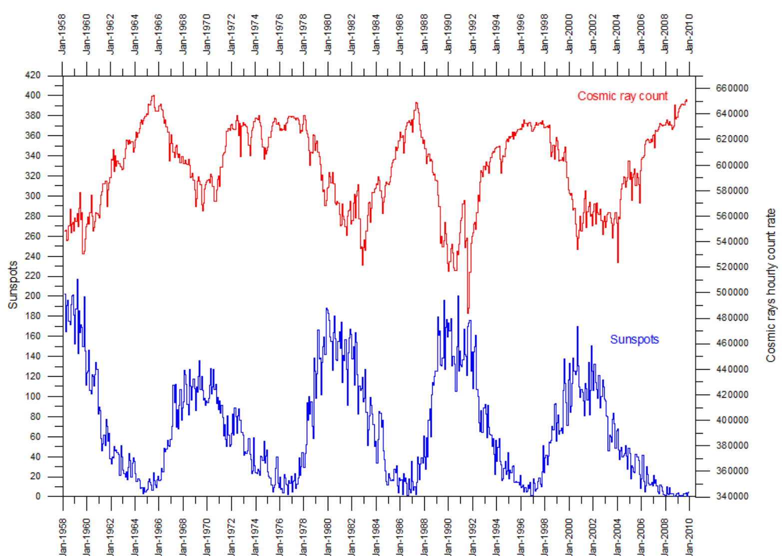

Variation of cosmic ray intensity (from Neutron Monitor data) and monthly sunspot activity

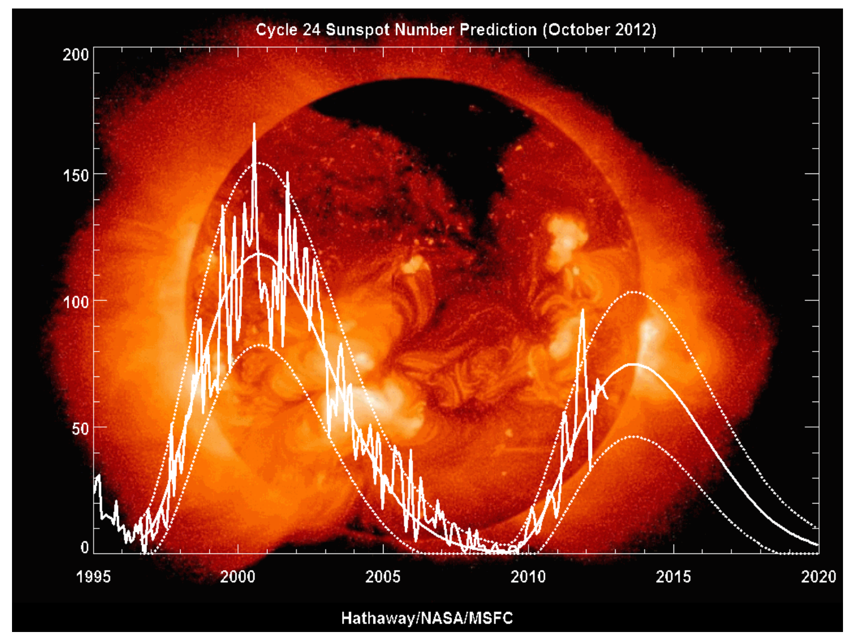

Variation of solar activity 11 years cycle

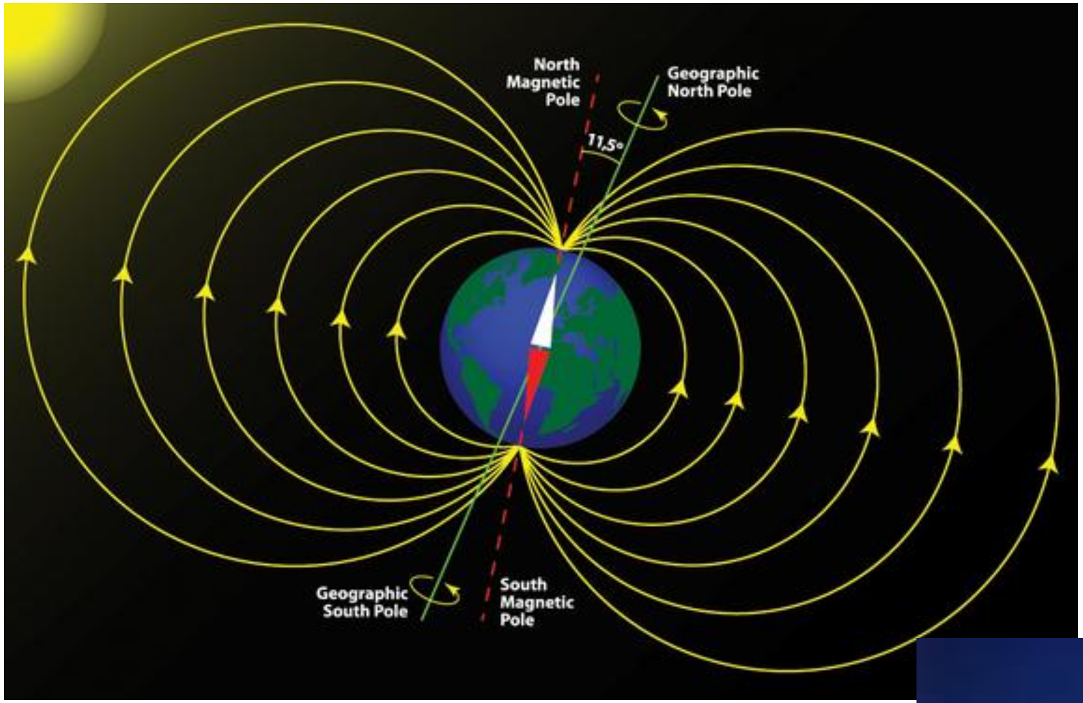

High altitude:
reduced atmosphere layer

High latitude:
Converging magnetic field lines

Space exploration…but

Risk for the health: *humans are exposed to a complex mixed radiation field*

- In space
- in high altitude flights
- In high altitude countries
- In high latitude countries

.

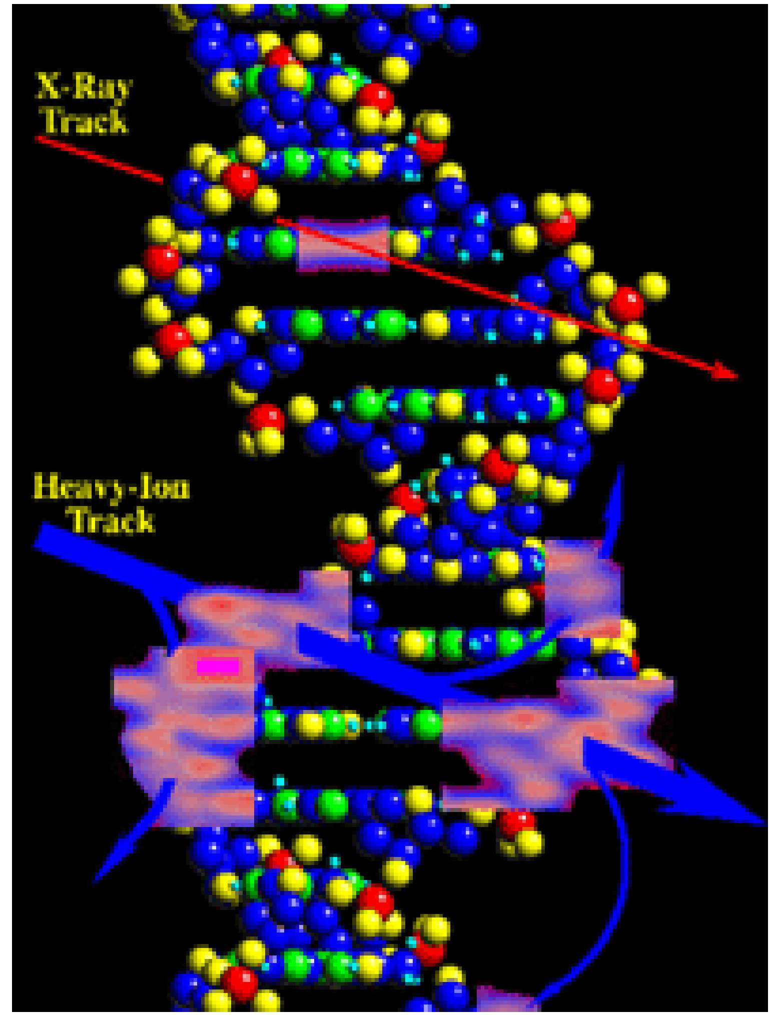

Qualche dato…

Per ricevere una dose di 1 mSv

17 mesi a Parigi

6 mesi in luoghi a grande altitudine

7 voli andata e ritorno Parigi-Tokyo

13 voli andata e ritorno Parigi-New York sul Concorde

1 ½ giorni a bordo della MIR (400 km di altezza)

Per un dato volo, la dose totale della radiazione cosmica ricevuta è direttamente proporzionale alla durata dell'esposizione, e quindi alla durata del volo.

10 yr Career Exposure Limits - NCRP Report n. 132 (2000)

Age	Male (Sv)	Female (Sv)
25	0.7	0.4
35	1.0	0.6
45	1.5	0.9
55	3.0	1.7

Anatomical Location	NCRP Report n 132 (2000) (Gy-Eq) 1 year limit
Eye	2.0
Skin	3.0
BFO	0.50

RADIATION DOSIMETRY

ADSORBED DOSE

Energy per Mass unit

1Gy = 1J / 1kg

$$\boxed{D = \frac{d\bar{\varepsilon}}{dm}}$$

DOSE

$$\boxed{D_T = \frac{d\bar{\varepsilon}}{dm_T}}$$

DOSE to a Tissue (or Organ)

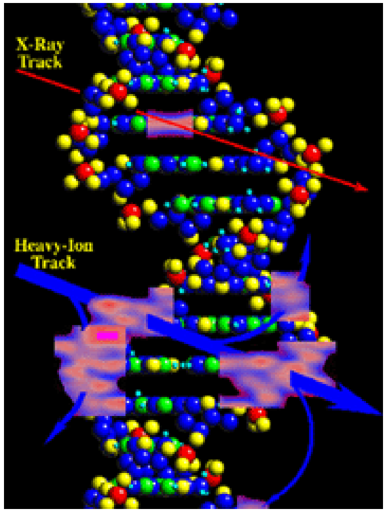

Ogni componente della radiazione ha una diversa efficacia biologica relativa. Per tenerne conto è necessario calcolare la DOSE EQUIVALENTE nel tessuto.

DOSE EQUIVALENT [Sv]

$$\boxed{H_T = \sum_R w_R D_{T,R}}$$

EFFECTIVE DOSE [Sv]

$$\boxed{E = \sum_T w_T H_T}$$

REFERENCE QUANTITY

w_R Radiation Weighting Factors

w_T Tissue weighting Factor

A organi diversi sono associati rischi diversi di effetti stocastici. Per considerare anche il tipo di tessuto, si calcola la DOSE EFFICACE.

L'energia ceduta da una particella al mezzo assorbente a causa di collisioni è misurata dal **LET,**

$$L = \frac{d\bar{\varepsilon}}{dl}$$ LET

Lineal Energy Transfer. [J / m.]

Nei problemi di radioprotezione si deve anche valutare la dipendenza dall'energia per gli ioni leggeri e pesanti.

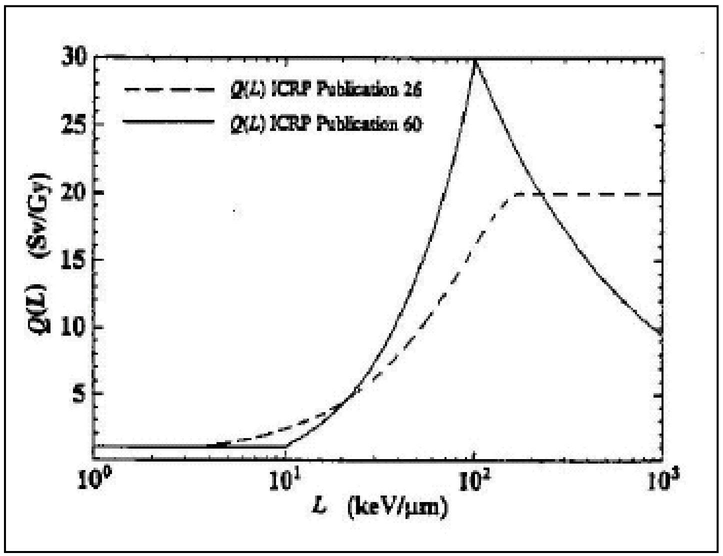

Quality Factor Q(L) as a function of LET

Si fa perciò ricorso al FATTORE DI QUALITA' Q della radiazione, che è una funzione del LET.

H* Ambient DOSE EQUIVALENT

$$H = \int Q(L)\, D(L)\, dL$$

Dose distribution of space radiation

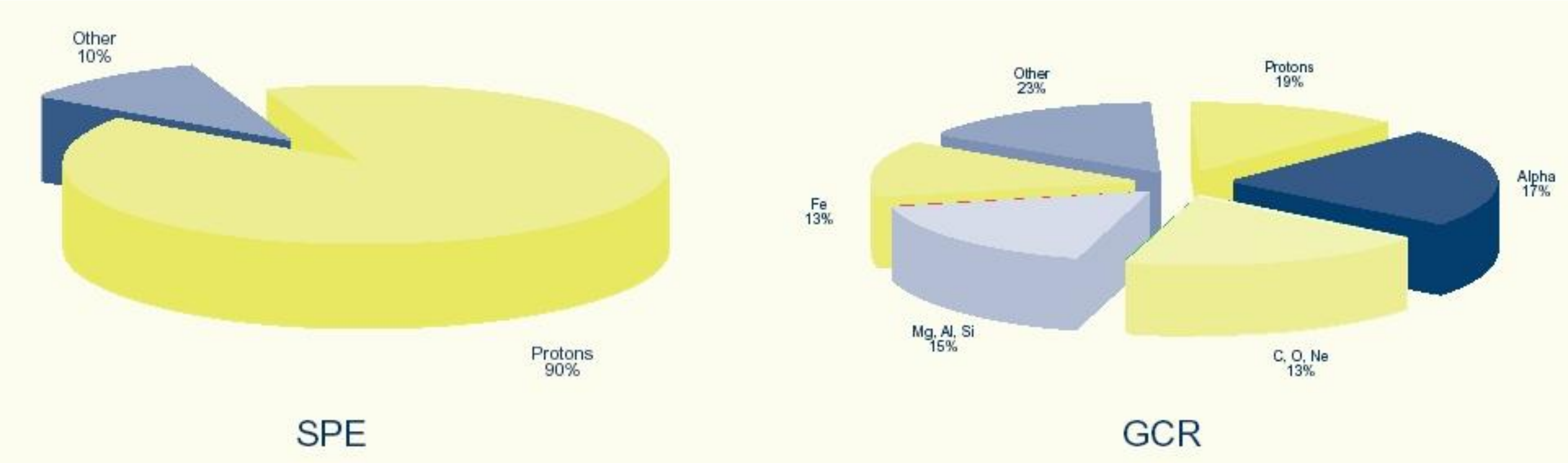

Relative contribution of different components of space radiation to the dose. The equivalent dose is evaluated at the skin, assuming exposure during the solar minimum behind a 5 g/cm^2 aluminum shield. (*ref. NASA: Strategic Program Plan for Space Radiation Health Research (1998*))

Secondary Neutrons in Atmosphere

Neutrons in atmosphere arise from:

1. interaction of primary cosmic rays with O and N atmosphere nuclei;

2. nuclear decays like:

$\Lambda \rightarrow n + \pi^0$

$\Sigma^+ \rightarrow n + \pi^+$

$\Sigma^- \rightarrow n + \pi^-$

Most of the thermal neutron in atmosphere are absorbed in such processes a

$^{14}N + n \rightarrow {}^{14}C + {}^{1}H$

5% of neutron having energies greater than 4 MeV take part in the reaction:

$^{14}N + n \rightarrow {}^{12}C + {}^{3}H$

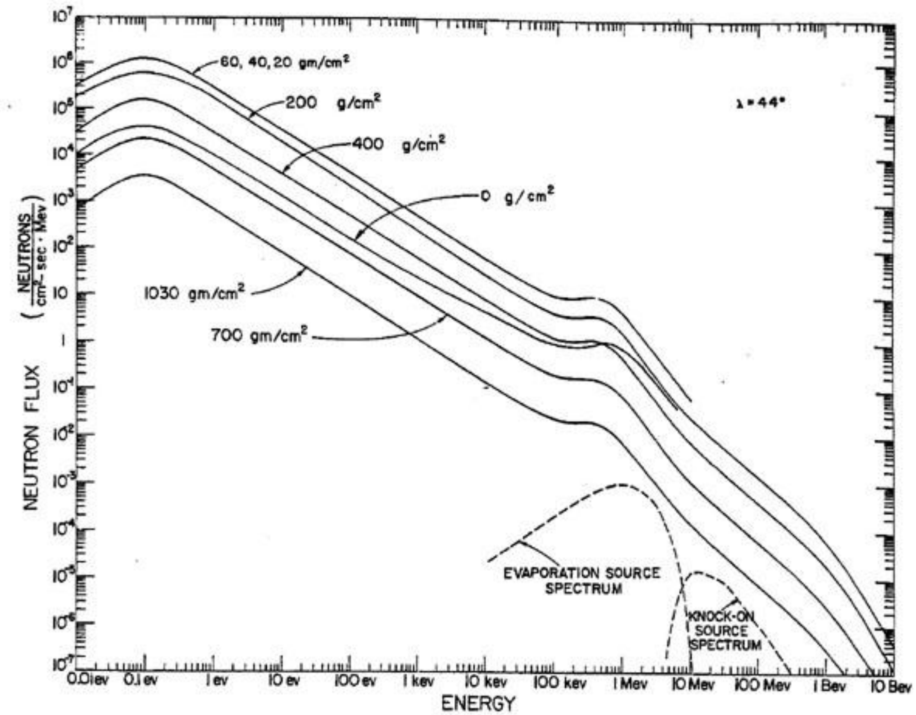

M. C. simulations and experimental data at various altitudes and latitudes in atmosphere

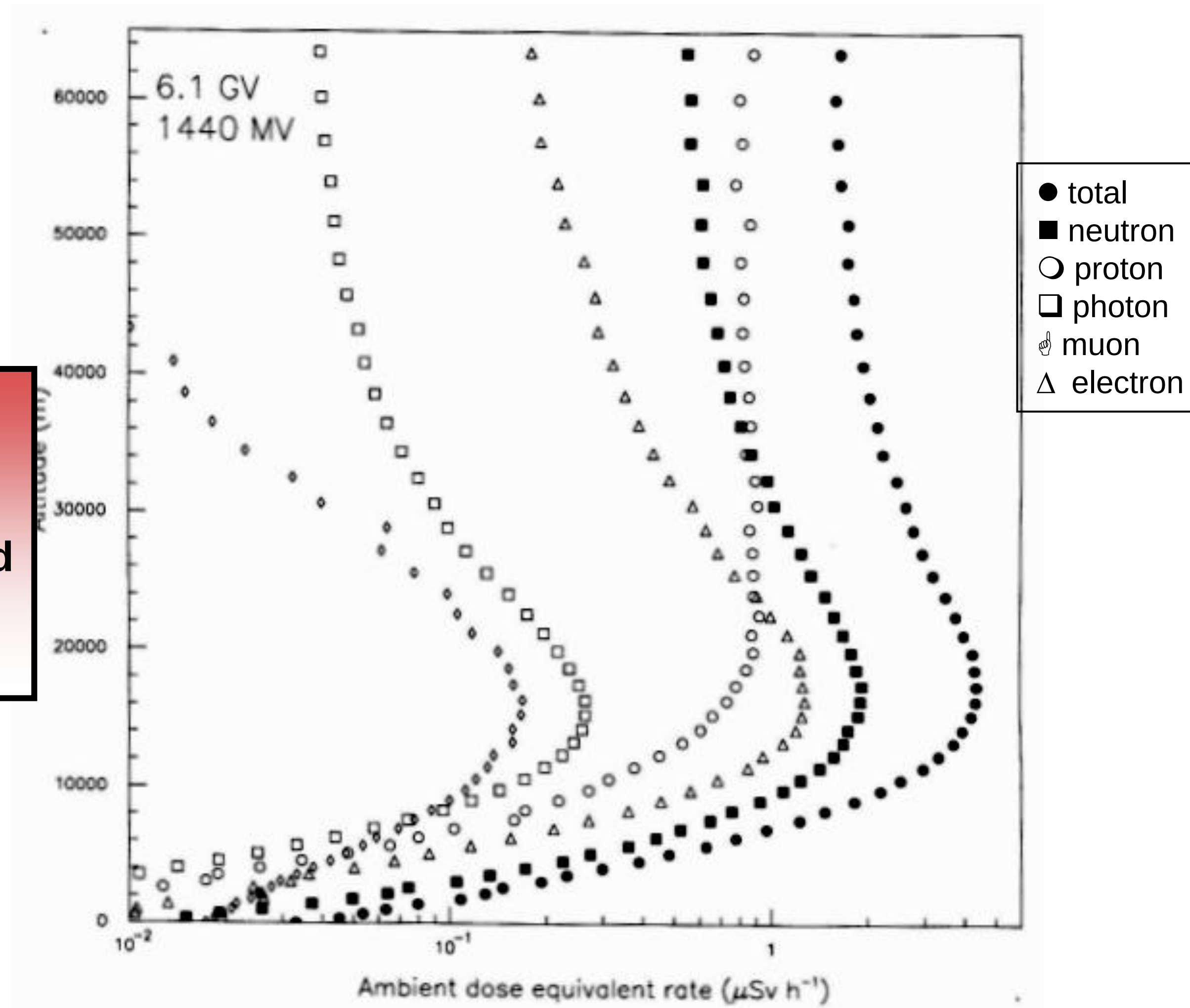

High latitude and maximum solar activity:
Ambient dose equivalent rate for different particles calculated using the FLUKA code.
(M. Pelliccioni)

Neutron Dosimetry

Types of radiations and energy intervals	Weighting factors of radiation, W_R
Photons, all energies	1
Electrons, all energies	1
Mesons, all energies	1
Neutrons energies	5
< 10 keV	10
10 – 100 keV	20
100 keV – 2 MeV	10
2 – 20 MeV	5
> 20 MeV	
Protons	5
Heavy Ions	20

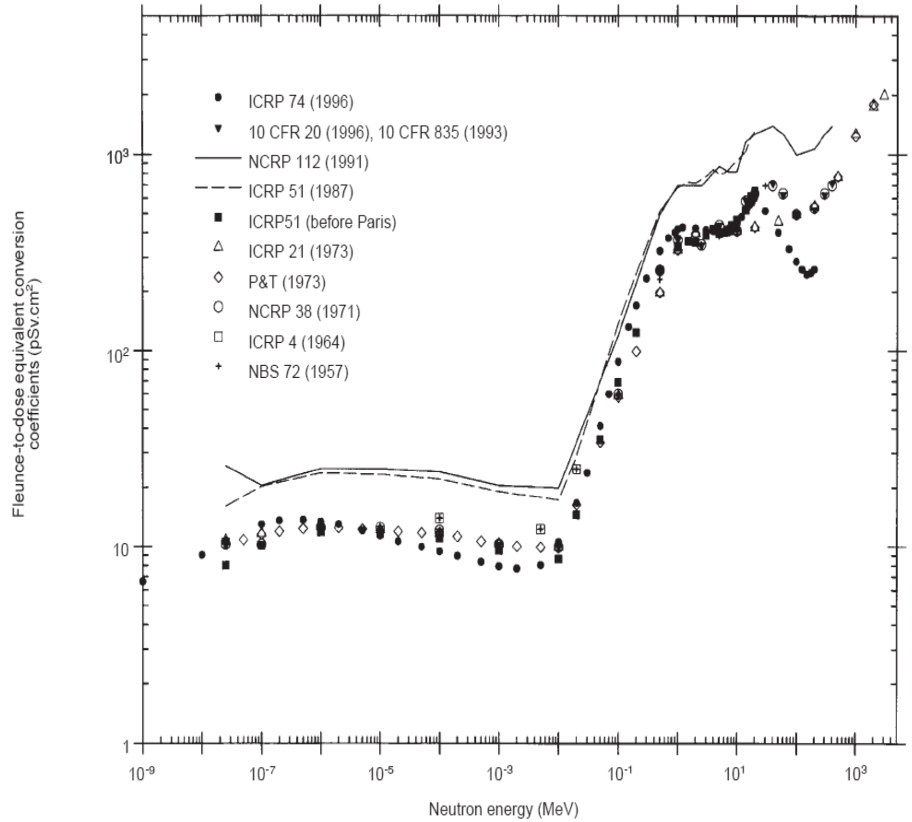

Neutron Conversion factors from fluence to ambient dose equivalent $(mSv.cm^2)$

It is evident that weighting factors strongly depend from neutron energy.
As a consequence, to evaluate accurately the neutron dose, it is required the evaluation of neutron energy spectrum, that for atmospheric secondary neutrons, extended from thermal energies to hundred of GeV. For this reason the assessment of neutron dose requires different detectors in different energy range.

Neutron component

- Neutrons are produced as secondary radiation by interaction of primary cosmic rays with the spacecraft shielding , togheter with other secondary particles (as protons and ions).
- The evaluations of neutron component of the radiation environment in spacecraft, both in LEO orbits and in deep space is of great importance because of their high LET.
- In view of long term manned or unmanned space missions, (mission to Mars, solar system exploration) neutrons can produce dramatic damages to the astronaute health and the on board instrumentation.

Neutron dose evaluation

An accurate neutron dose evaluation is very complex because:

- Fluence to dose equivalent conversion factors strongly depend from neutron energy.
- For an accurate dose evaluation it is necessary to know the neutron energy spectrum.
- Secondary neutron energy range varies from thermal energy (0.025 eV) to hundred of GeV
- Different detectors are required , based on different physical effects
- The detector responses are elaborated by using a mathematical unfolding code

Fluence to neutron dose equivalent conversion factors

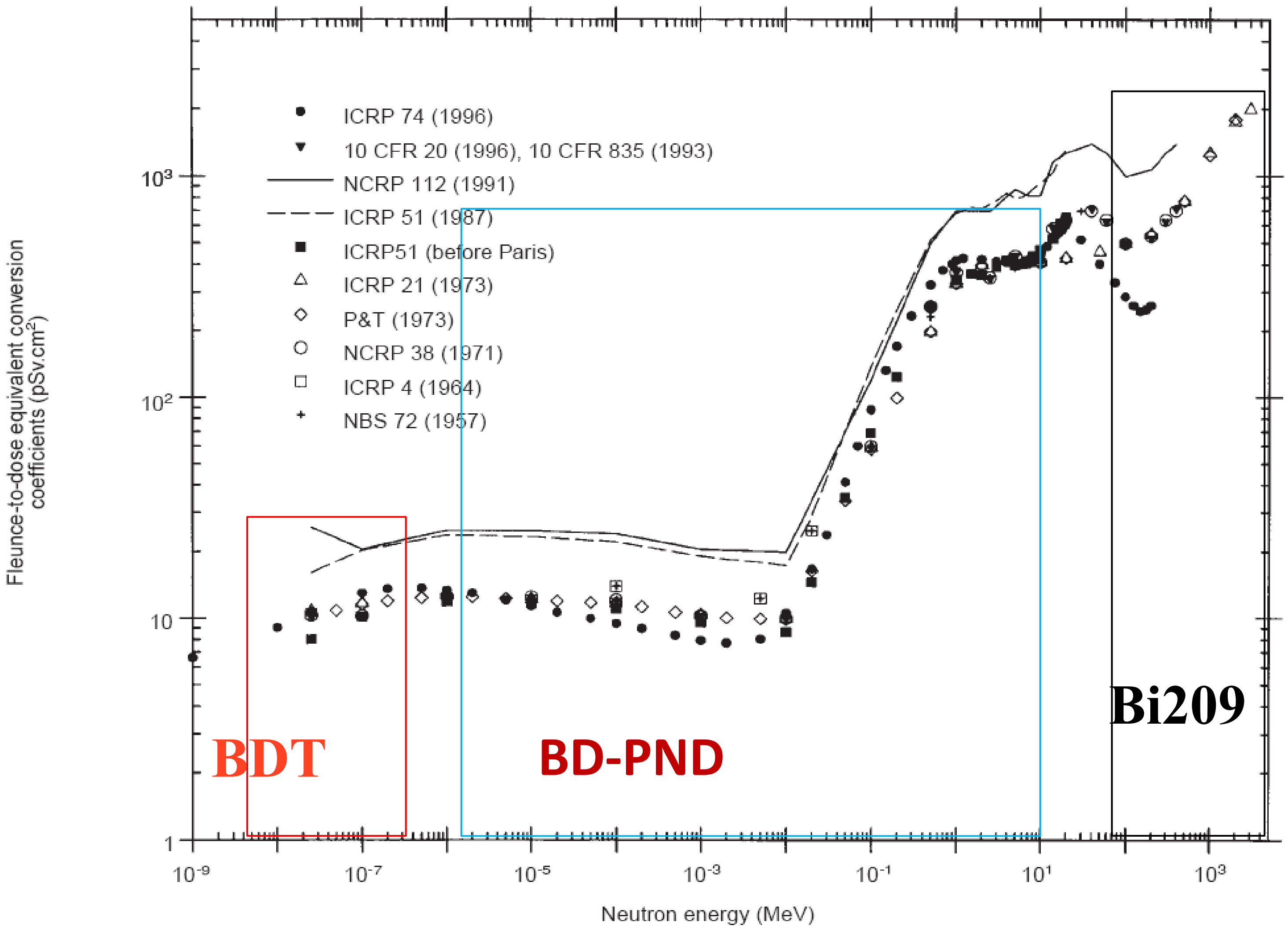

Passive Neutron detectors

1- Bubble detectors

The detector is constituted by a vial filled with a tissue-equivalent polymer, in which drops of a superheated liquid (freon) are dispersed.

- Two different types of detectors, with different chemical composition of the liquid, different threshold and energy response are available

  BDT low energy neutrons (0.025 eV – 0.4 eV)

  BD-PND high energy neutrons (100 keV-20 MeV)

- The system works using the superheated drop detector mechanism: the charged recoils particles produced by the interaction of neutrons with the polymer nuclei transfer their energy to the superheated drops, which become bubbles trapped in the gel. Their number is related to the neutron dose, according to the factory calibration.

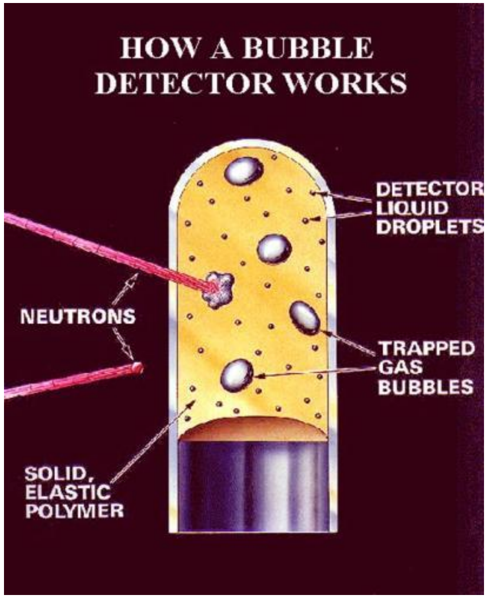

Bubble detector working scheme

Neutron spectrometer (1)

BTI (Bubble Tech. Ind., Ontario, Canada)

SHORT ENERGY RANGE 0.025 eV (Thermal)- 20 MeV

1. **BDS 10** — **10 keV - 20 MeV**
2. **BDS 100** — **100 keV - 20 MeV**
3. **BDS 600** — **600 keV - 20 MeV**
4. **BDS 1000** — **1 MeV - 20 MeV**
5. **BDS 2500** — **2.5 MeV - 20 MeV**
6. **BDS 10000** — **10 MeV - 20 MeV**

Six different types of superheated drop detector, with different chemical compositions, different thresholds and energetic responses

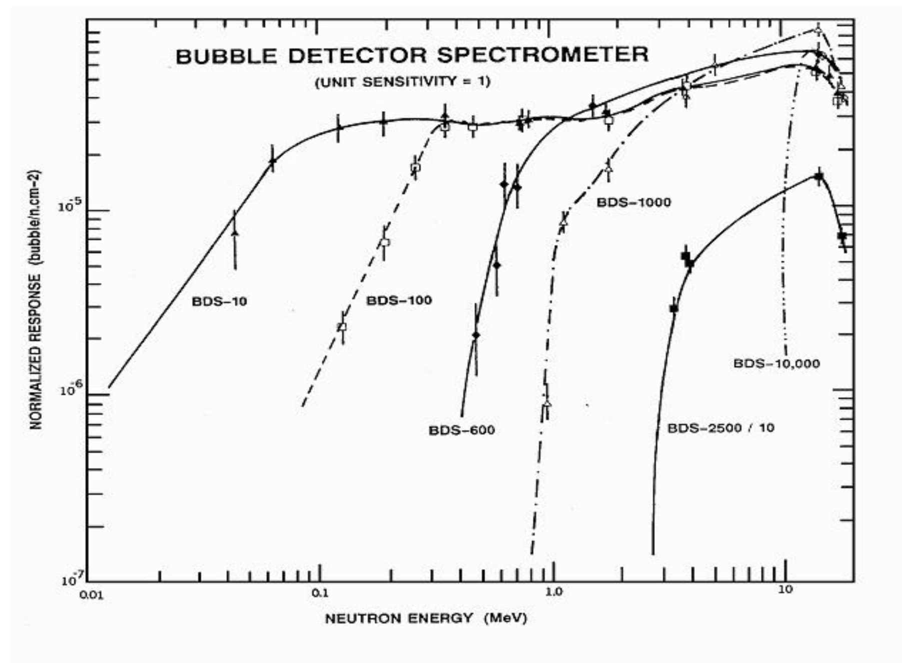

Three response curves sets in correspondence of different temperatures values (20 °C, 25 °C, 30 °C, 32.5 °C, 35 °C)

Passive Neutron detectors

2- ^{209}Bi detector (100MeV-400 GeV).

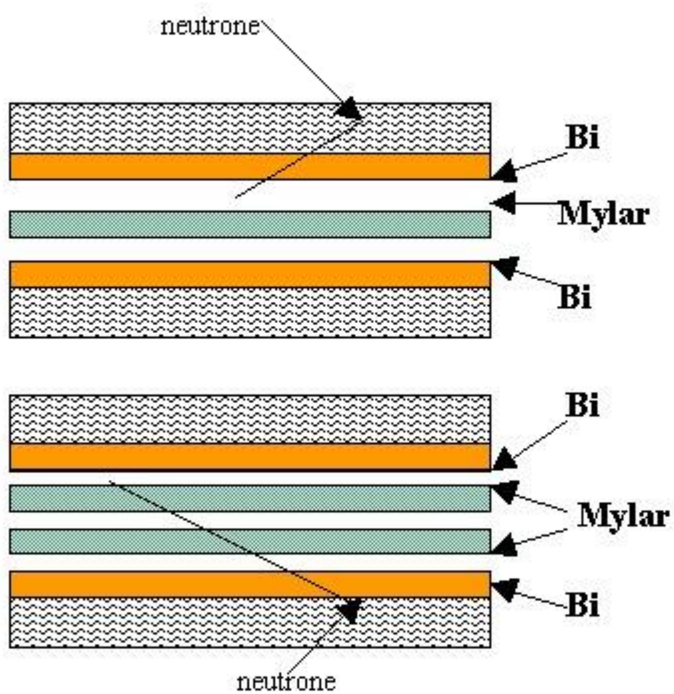

Bismuth detector scheme

The Bismuth stack consists of alternate mylar (0.125 mm) and bismuth layers (0.025 mm) . When the neutron crosses the stack, a fission event can occur in the bismuth layer, generating fission fragments that produce a track damage in the mylar layers.

Tracks can be counted after electroetching, and their number is related to the high energy neutron dose, following the detector response curve

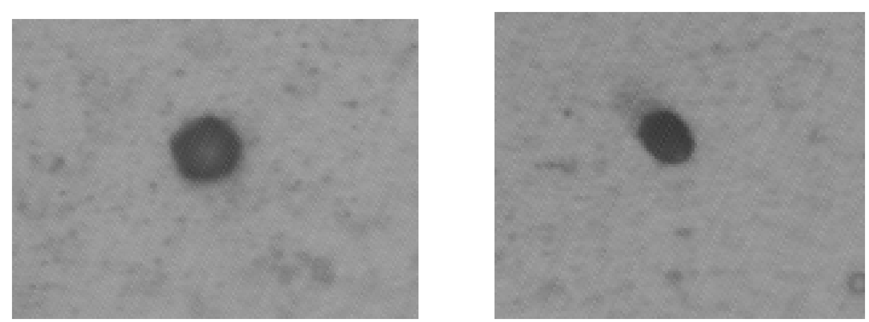

An exemple of neutron tracks on mylar after electro-etching.

The BUNTO unfolding code

It is based on BUNKI's algorithm (SPUNIT), which finds the not negative solution through a iterative perturbation procedure.

It can find a solution using a starting information on the spectrum shape, but it can also work in lack of information on the initial spectrum.

The solution $\boldsymbol{\Phi_E(E)}$ is the calculated mean from a number of spectra obtained by a random generation of $\boldsymbol{M_j}$ sampled on a normal distribution, whose parameters $\boldsymbol{m}$ and $\boldsymbol{s}$ are the final value and the associated uncertainty of the $\boldsymbol{j^{th}}$ detector.

R_j : detector reading
A_{ij} : response curve values
Φ_i : neutron fluence (to be determined)
m : number of energy threshold
n : number of energy intervals

$$R_j = \sum_{i=1}^{n} A_{ij}(E)\Phi_i(E) \qquad j = 1..m$$

It can be used with different spectrometry systems,
if the response matrix of the detectors is known.

Calibration

- The calibration of the passive detector system has been performed at CERN (T14 position, H-6SPS beam): this facility is a reference field for the calibration of neutron detection systems to be used in the cosmic ray field.

- The passive detector results, unfolded with the BUNTO code, are compared with the MC simulation of the experimental setup; the results are consistent.

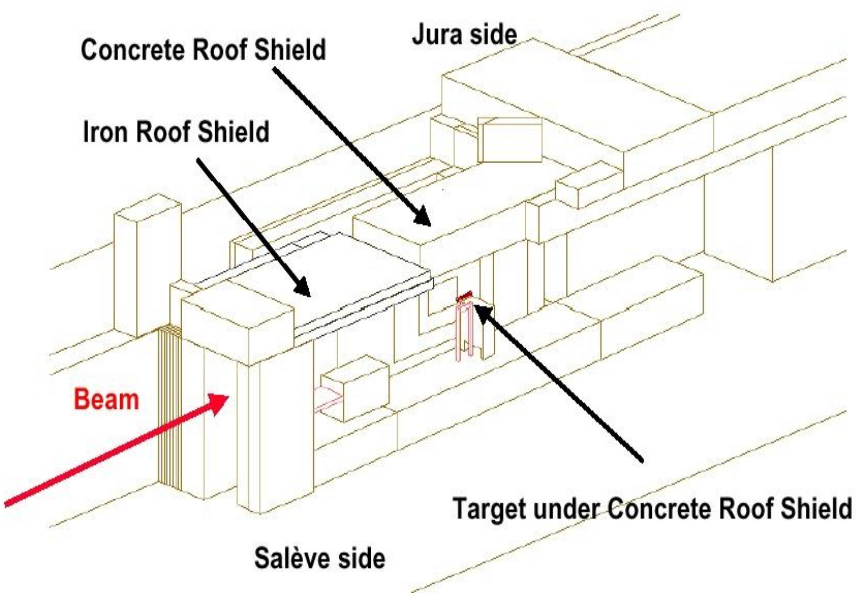

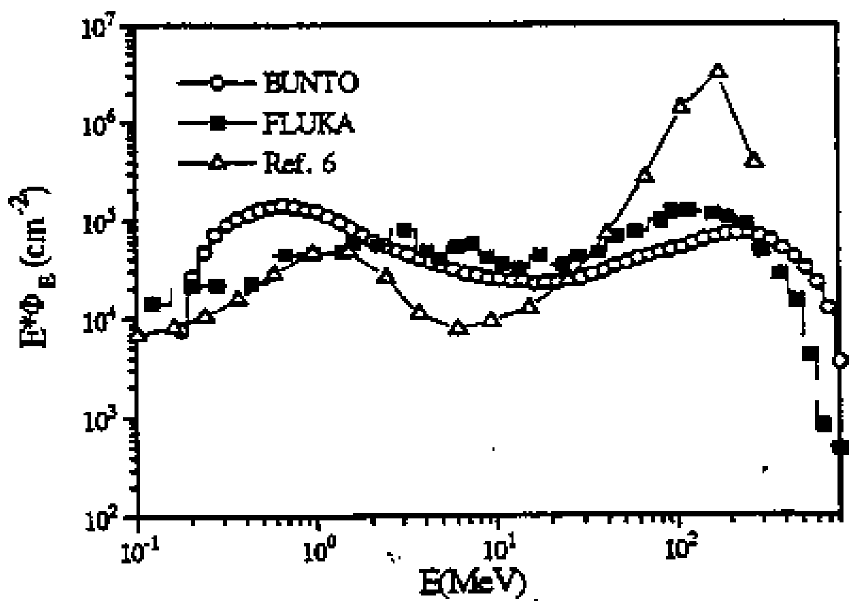

Neutron Dosimetry
(INFN - ALITALIA - ASI - ESA –NASA projects)

1. **High mountain laboratories**
   Plateau Rosa, Testa Grigia Laboratory
   h=3480 m,
   45° 56’ 03’’ N, 7° 42’ 28’’ E
   Chacaltaya, La Paz (Bolivia)
   h=5400m, 16°S

2. **Alitalia flights** AZ784/11, AZ784/12
   Roma-Tokyo-Roma
   h=11500m,
   35° 45’ 9’’ N, 14° 23’ 2’’ E
   68° 30’ 5’’ N, 7° 33’ 4’’ E

3. **ASI balloon flights**
   Base Trapani Milo, Trapani-Siviglia
   h=38000m,
   36° N

4. **ESA project**
   BIOPAN on Foton M1 satellite

5. **ISS June 2011** BIOKISS project

Neutron spectrometry (100 keV-400 GeV) with passive detector

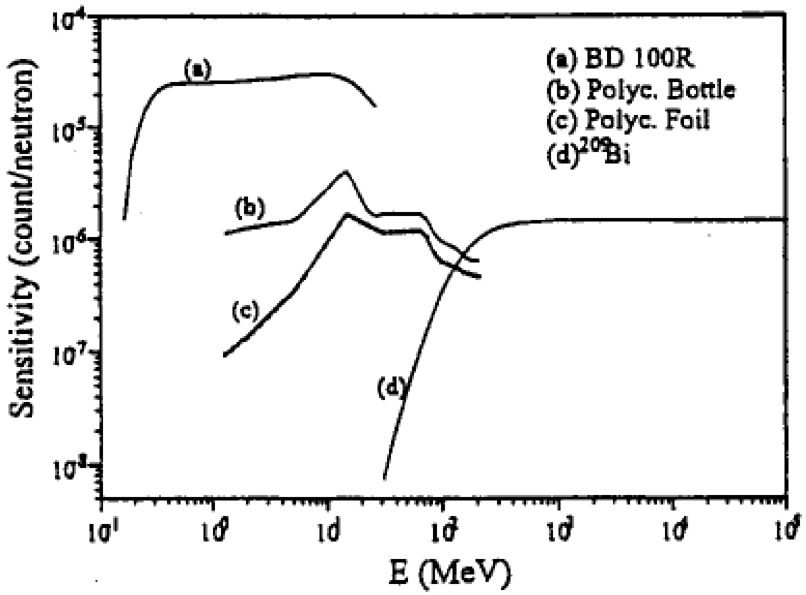

Detector responses

a)Bubble detector BD-PND **(100KeV-20MeV)**

b) Polyc. bottle **(1MeV – 100MeV)**

c) Polyc. foils **(1MeV – 100MeV)**

d) Fission Bismuth detector **(100MeV-400GeV)**

Unfolding code BUNTO

$$R_j = \sum_{i=1}^{n} A_{ij}\Phi_i \qquad j = 1..m$$

R_j : detector reading
A_{ij} : response curve values
Φ_i : neutron fluence (to be determined)
m : number of energy threshold
n : number of energy intervals

Unfolded spectra

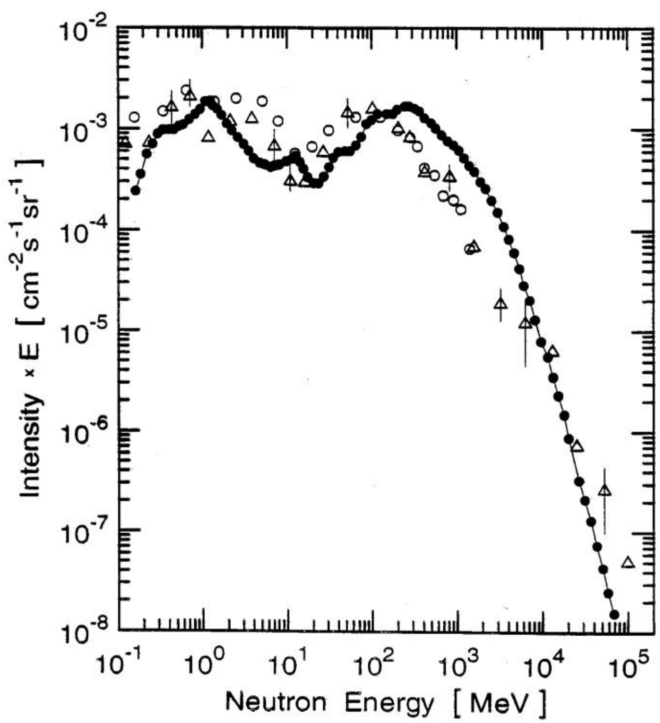

Matterhorn –Testa Grigia 3600 m

Neutron spectra at various altitudes and latitudes

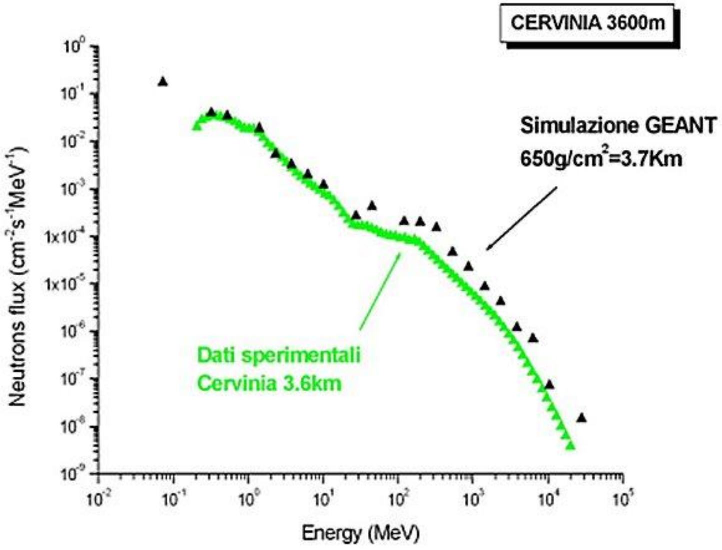

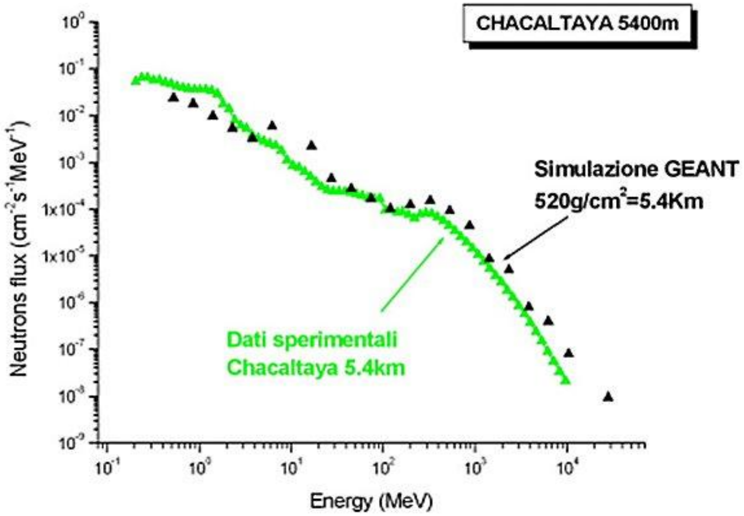

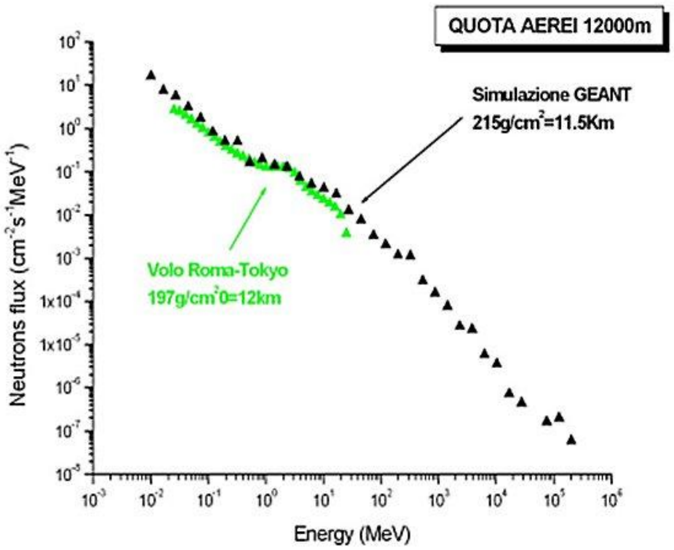

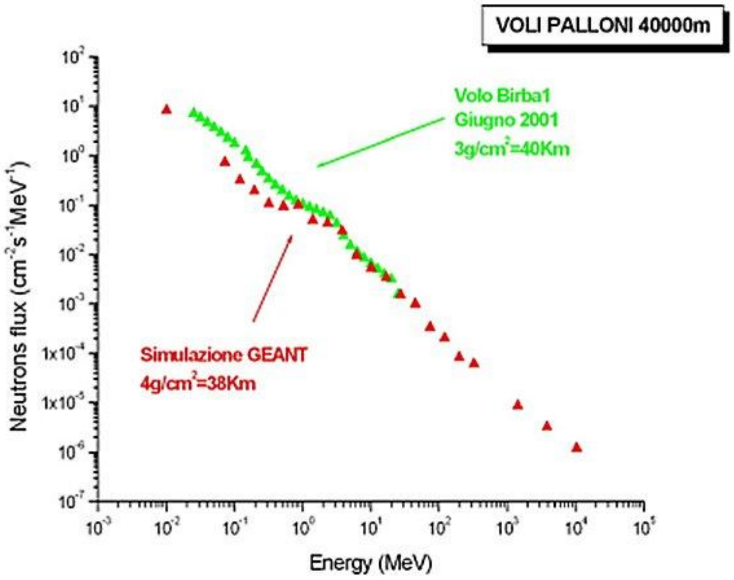

Intercontinental Flights

Alitalia: Roma-Tokyo
Roma – Buenos Aires

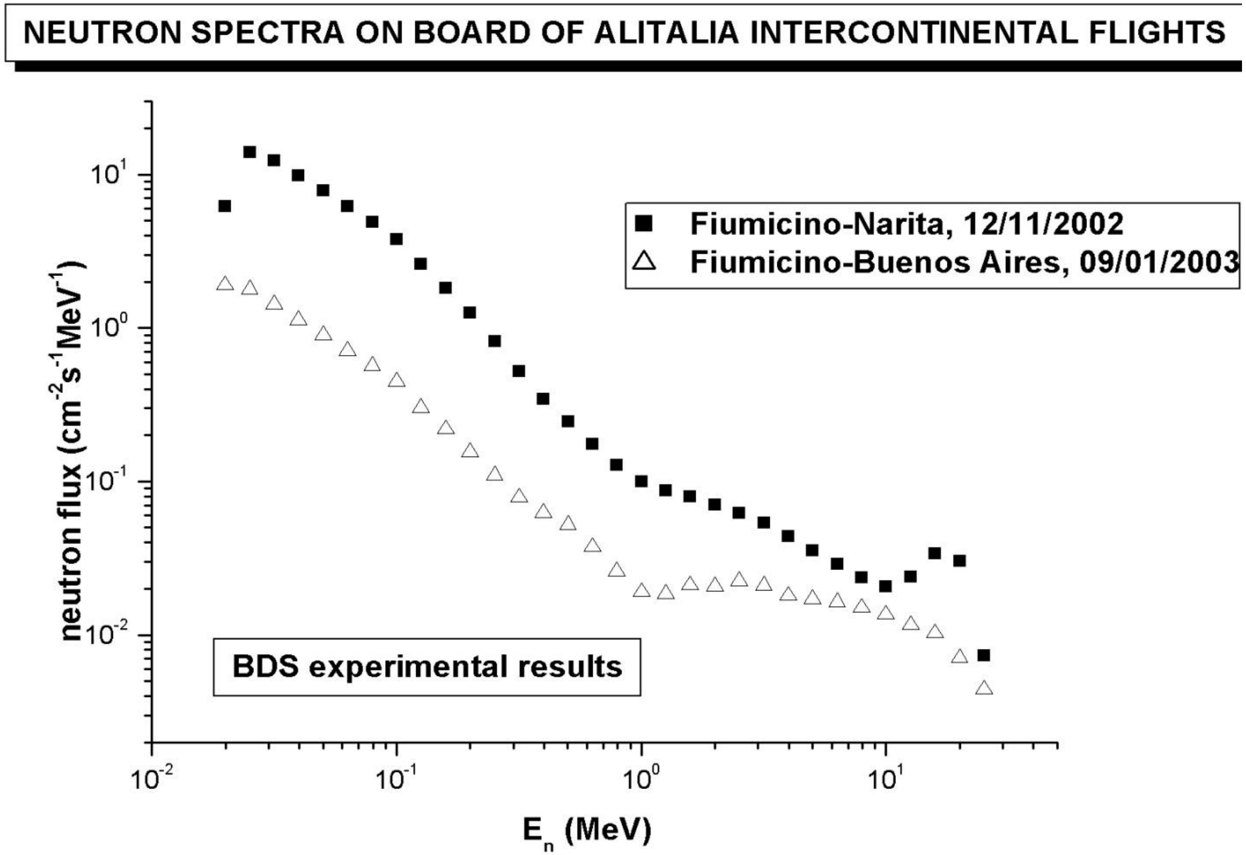

VOLO ASI BIRBA1
Trapani -Siviglia

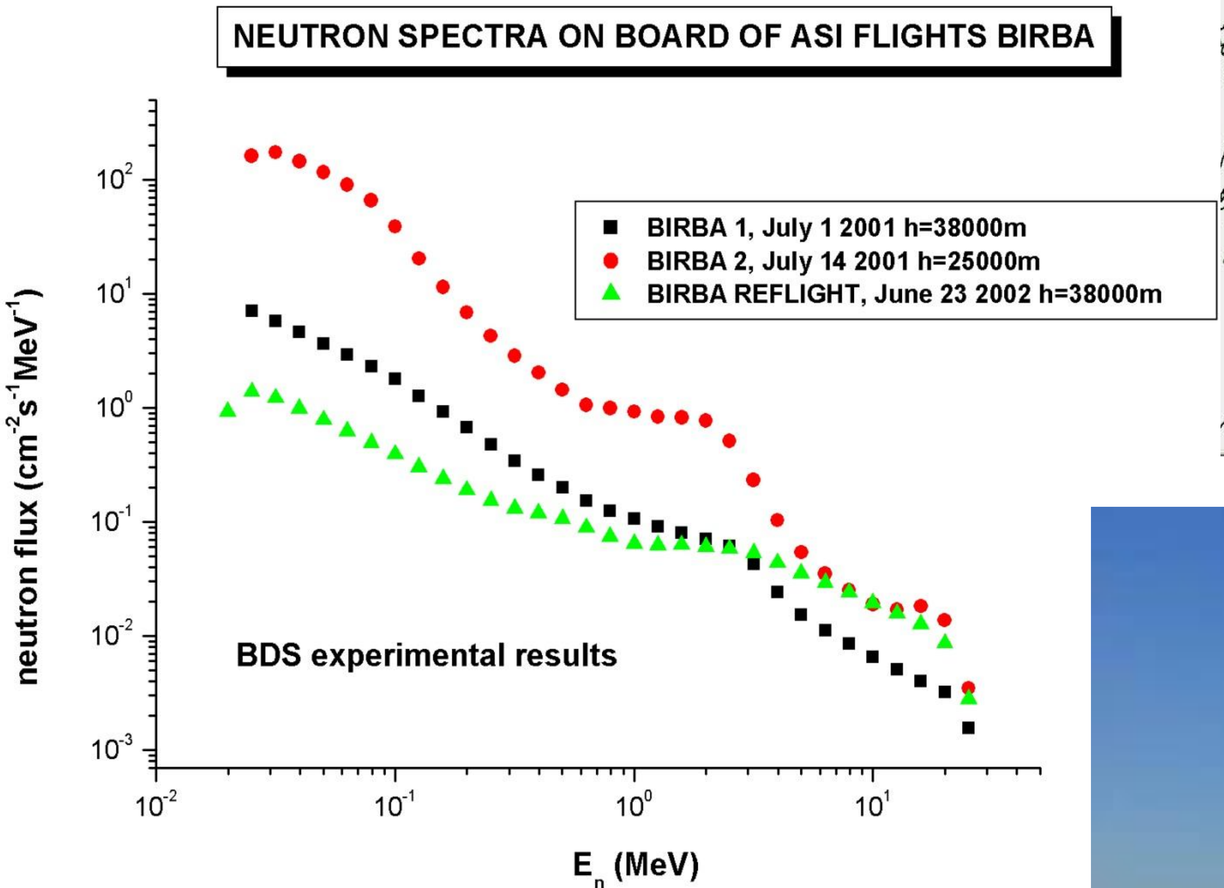

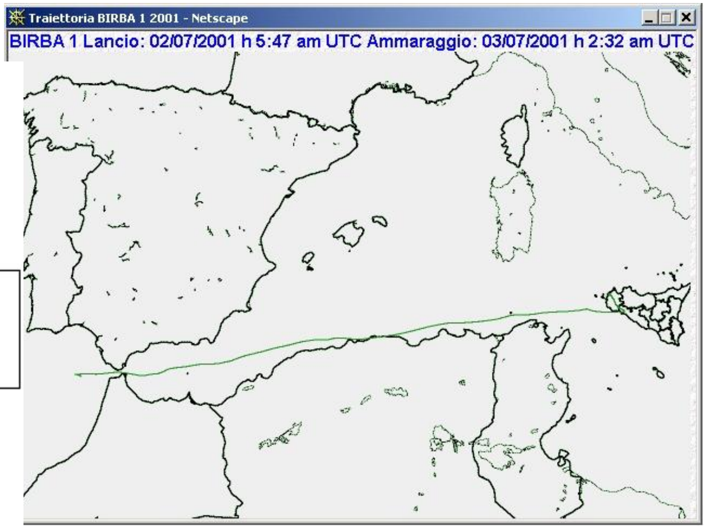

Experimental measurements

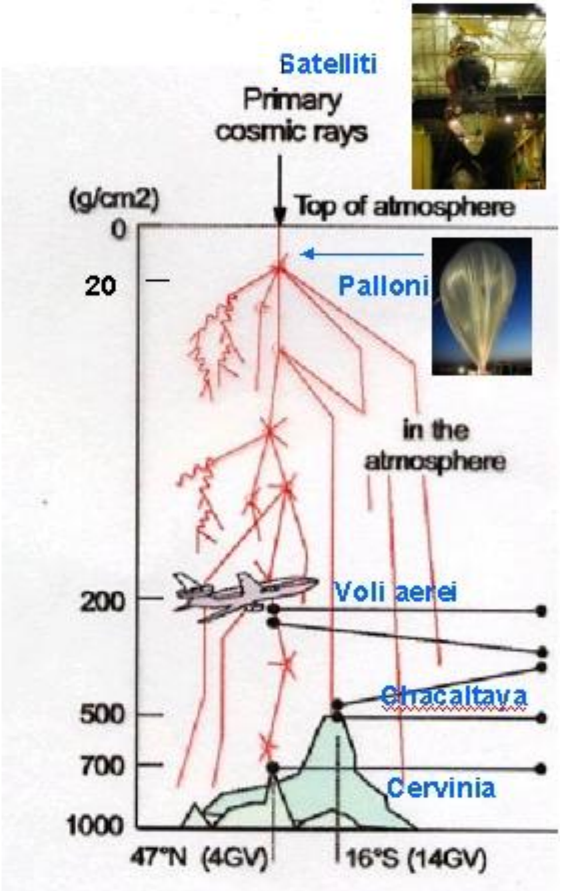

Disponibilità di dati a diverse quote

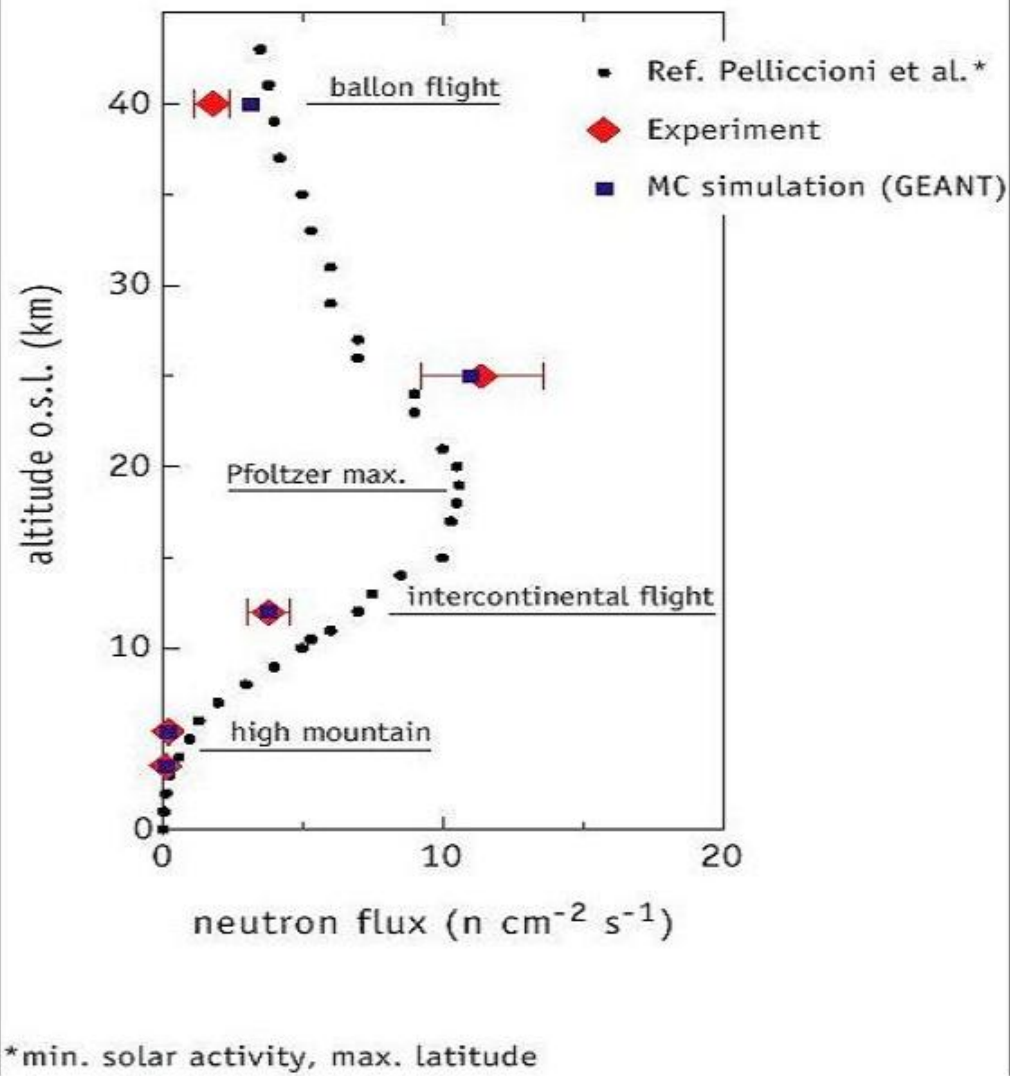

Instrumentation at Marambio Base

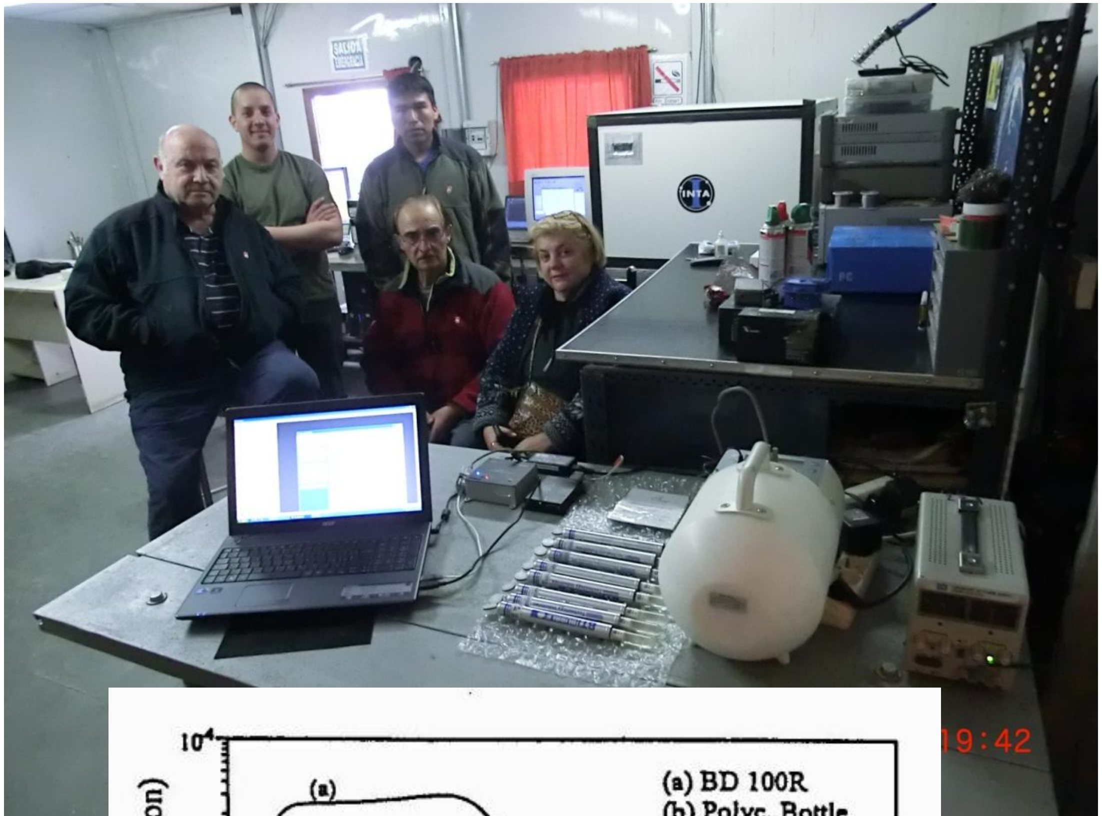

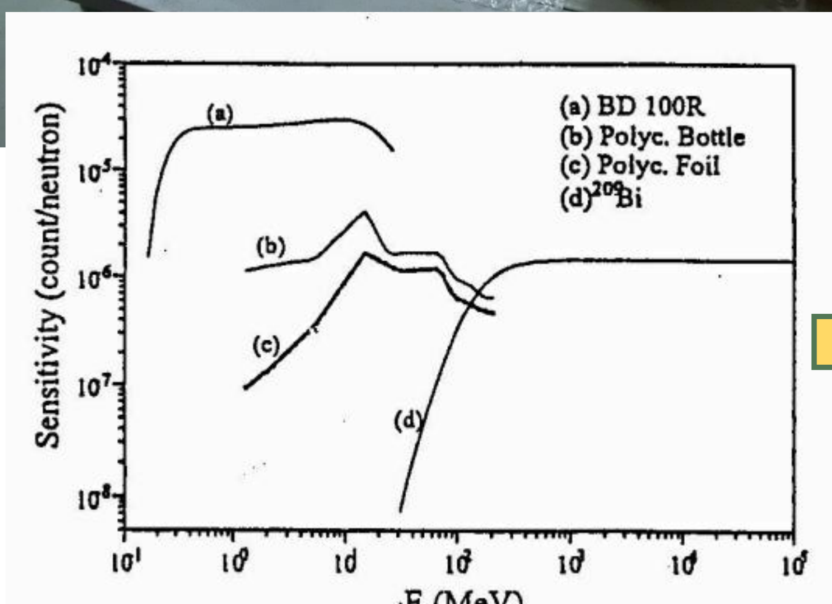

e.m. and charged particles
All energies
Liulin LET spectrometer

Bubble Detectors
BDT
0.025 eV-20 MeV
BD-PND
100 keV -20 MeV

Polycarbonate detectors
20 MeV - 100MeV

Bi209 stack
200 MeV-400 GeV

Rem Counter
0.025 eV-17 MeV

NEUTRONS

Pressure effect in Antartic

- **Relationship between cosmic-ray intensities and atmospheric pressure**

There is a relationship between the neutron dose rate and the atmospheric pressure in the monitoring period. The main component of the cosmic-ray measured at ground level is secondary cosmic-ray, and is attenuated by the air above the ground which acts as a shield. The cosmic-ray neutrons and the ionizing components measured at ground level vary according to an exponential attenuation law with the atmospheric pressure in the form of ~exp(-A·P).

$$\boldsymbol{N(Po + P) = N(Po)} \exp \boldsymbol{(-aP).}$$

- The largest deviations occur over Antarctica where ground level pressures are 20–40 hPa lower than the standard atmosphere at all altitudes. Secondary particle production rates in Antarctica are therefore 25–30% higher than values calculated by scaling Northern Hemisphere production rates with conventional scaling factors.

Passive Detectors (Neutron component)

WIDE ENERGY RANGE 0.025 eV (Thermal)- 400 MeV

Bubble dosemeter
BD100R 100keV - 20 MeV

Polycarbonate detectors
1MeV-100MeV

RESPONSE CURVES

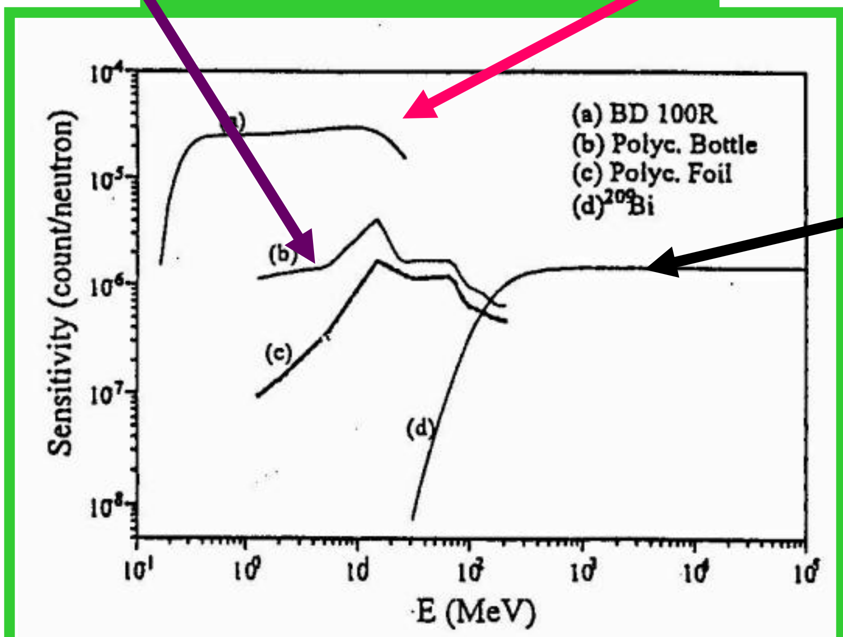

Fission detector ^{209}Bi
100MeV -100GeV

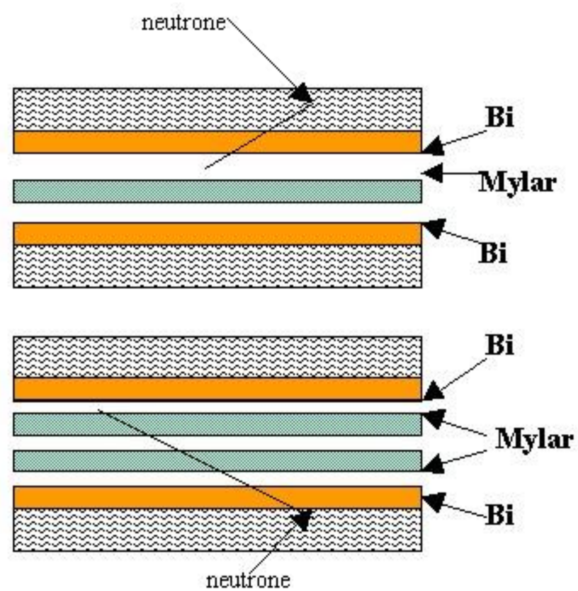

Active detectors

NEUTRONS

Rem Counter 2222

The Rem Counter neutron detector is constituted by a BF3 counter embedded along the center axis in a 30-cm-diameter and 32-cm-height paraffin cylinder ; the detector allows to measure the ambient dose equivalent rate and the integral ambient dose equivalent for neutron in the energy range **0.025 eV- 17 MeV.**
. The monitor shows the ambient neutron dose equivalent in terms of mSv/h and in terms of integral dose (mSv)

E. m and Low LET Charged particles

LIULIN LET spectrometer

LIULIN detector is constituted by one silicon semiconductor detector, one charge-sensitive preamplifier, 2 microcontrollers and a flash memory.

LIULIN is designed as a handy spectrometer-dosimeter for continuous monitoring of the radiation. After switching on, the instrument starts to measure in 256 channels the spectrum used to calculate the dose and the flux of particles in the silicon detector.

Pulse analysis technique is used for the measurement of the deposited energy in the detector in terms of Lineal Energy Transfer [J/m]

Instrument calibration

Liulin monitors the dose and the number of Energy deposition events in Si detector
The amplitude of the pulse is proportional to a factor of 240 mV/MeV of energy loss in Si.

The dose evaluation is calculated from

$$D = k\sum_{i=1}^{256}(E_i A_i) / m_d$$

D [mGy] is the dose i
E [J] - is the energy loss in the channel i
A is the number of events in the channel i
k is a coefficient depending on calibration field

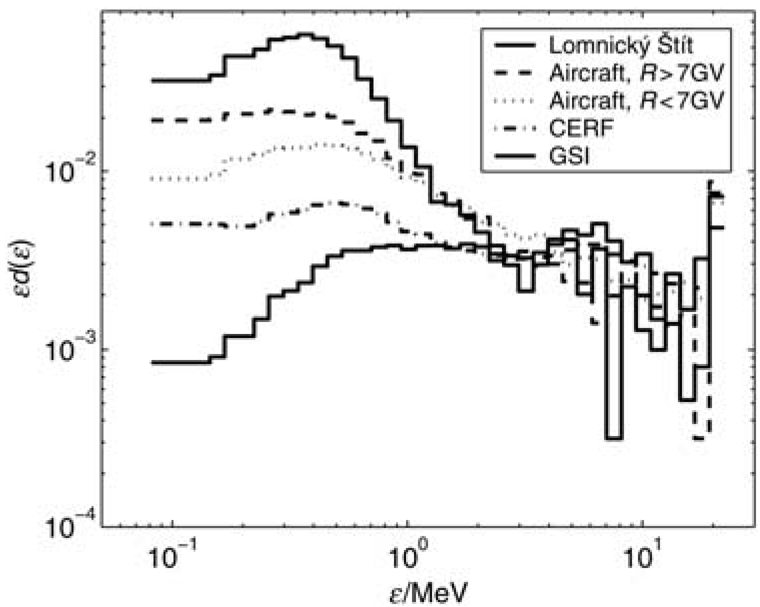

Figure 3. Energy deposition spectra measured with Liulin in different radiation fields.

The quantity **εd(ε)** is plotted as a function of the imparted energy

Where **εd(ε) = d(Dsi)/dε.**

$\mathbf{H^*(10)} = \boldsymbol{k_{Low}\, D_{Low} + k_{Neut}\, D_{Neut}}$

In this case Liulin4 it is no sensitive to neutrons

$\mathbf{H^*(10)} = \boldsymbol{k_{Low}\, D_{Low}}$

For e.m radiation and low LET charged particles (e+, e-, μ, π)

$\mathbf{H^*(10)} = \boldsymbol{D_{Low} = D_{Si}}$

Preliminary results

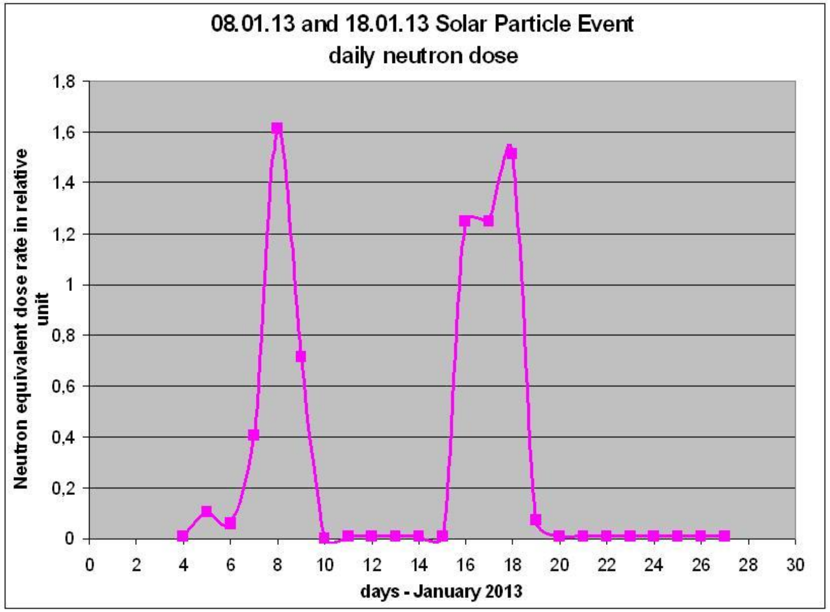

Fig.1 Daily mean neutron ambient equivalent dose rate measured by Rem -Counter 4th to 28th January 2013.

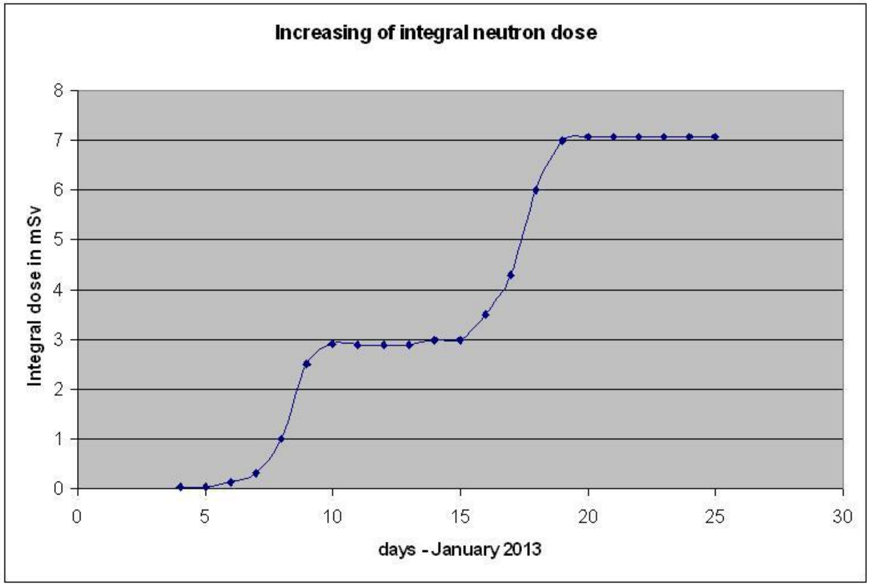

Fig.2 Integral neutron ambient equivalent measured by Rem –Counter

Are evident two very strong peak in correspondence of 8th and 18th of January, probably due to solar flares or Coronal mass ejection.

- **The dose rate increase sharply from 0.03 μSv/h to 50 μSv/h.**
- **The integral dose reachs 7 mSv**

January 2013 measurements

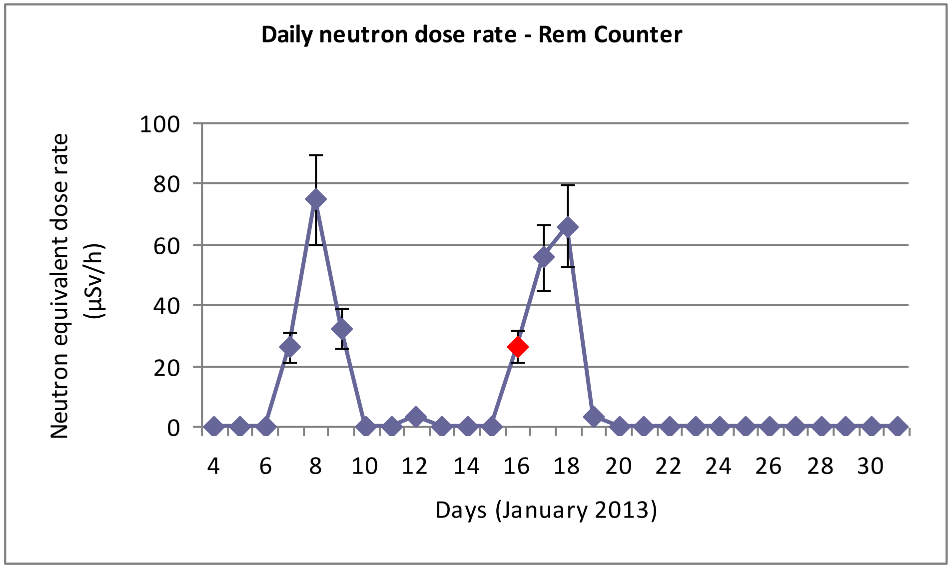

Rem Counter- Neutrons

-0.025 eV< En< 17 MeV

Fig 1a. Daily mean neutron ambient equivalent dose rates (μSv/h) measured by Rem-Counter is shown from 4th to 30th January 2013

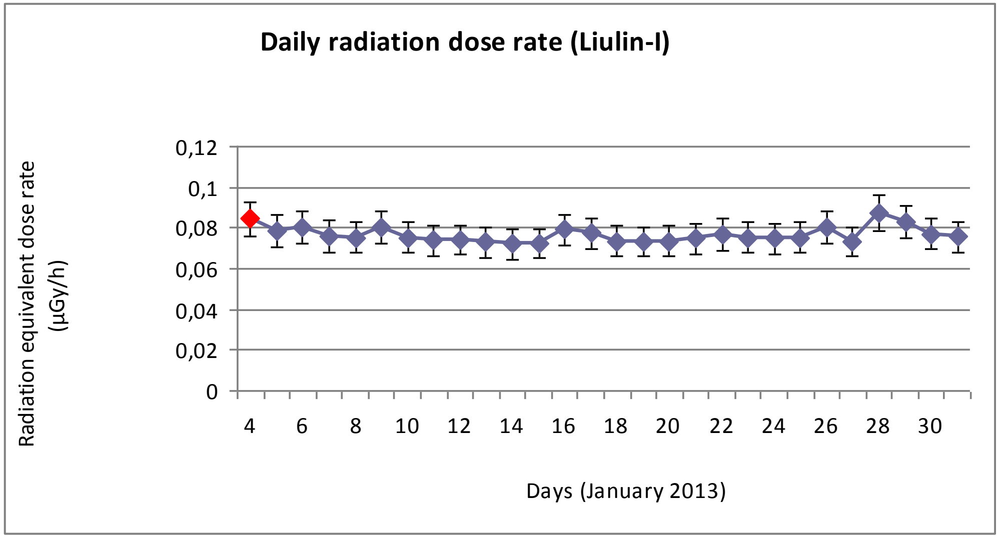

Liulin -Low LET - e.m,

Fig. 1b Daily mean radiation equivalent dose rates (μGy/h) measured by Liulin-I is shown from 4th to 30th January 2013.

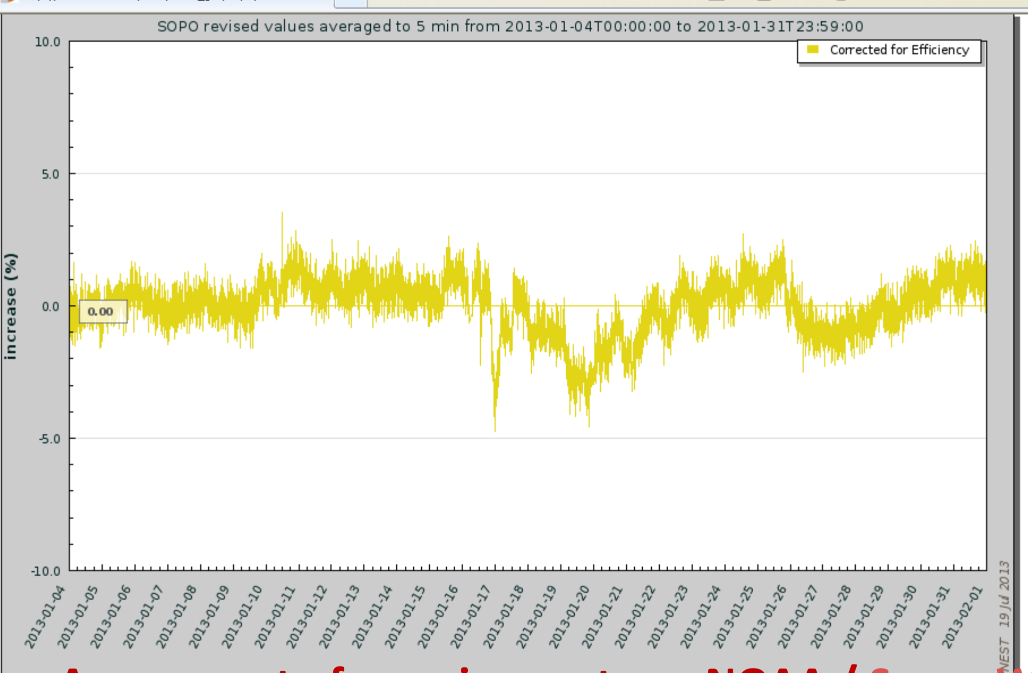

Neutron Monitor Database SOPO station

(http://www.nmdb.eu/nest/)

Assessment of cosmic events on NOAA / Space Weather Prediction Center

05 January: Activity increased to moderate levels due an impulsive M1 event observed at 05/0931Z from Region 1652.

11 January: moderate levels were reached as Region 1654 produced two M-class flares; M1 at 11/0911 UTC with associated Type II (537 km/s) and Type III radio bursts and an M1/1f at 11/1507 UTC.

13 January: moderate levels were reached as Region 1652 produced two M-class flares; M1 at 13/0050 UTC with associated Type II (649 km/s) and Type IV radio sweeps as well as Earth-directed CME. Bz component of the interplanetary magnetic field switched from maximum values of approximately +10 nT to -14 nT indicative of the arrival of 13 January CME.

16 January: CME at 16/1900 UTC, likely associated with filament eruption near Region 1650. A greater than 10 MeV proton enhancement was observed at geosynchronous orbit beginning late on 16 January, peaked at 2 pfu at 17/1715 UTC and declined to background levels by 18/0600 UTC. A corresponding sudden impulse was observed in the Boulder magnetometer (21 nT) at 19/1733 UTC). The shock arrival was consistent with the arrival of a glancing blow from the 16 January CME.

February 2013 measurements

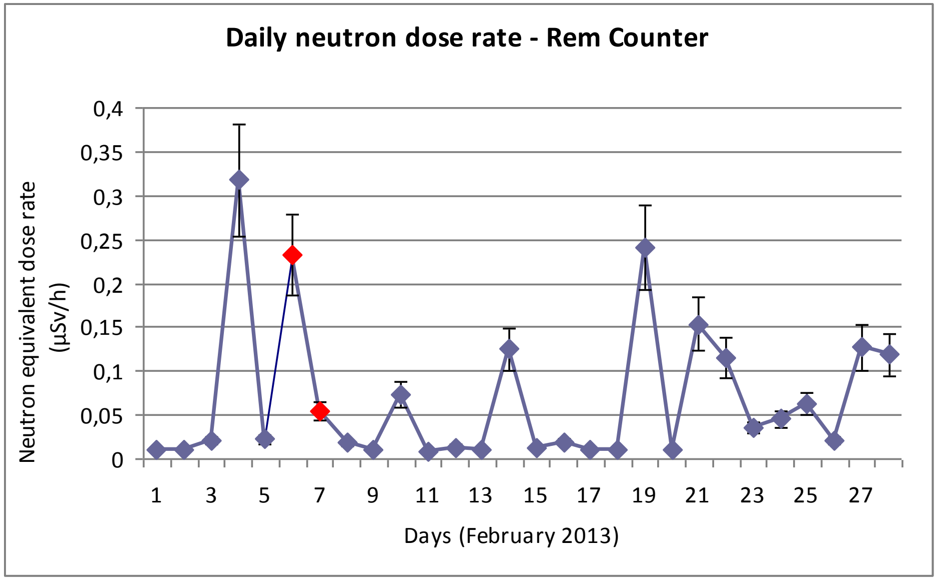

Rem Counter- Neutrons

-0.025 eV< En< 17 MeV

Fig. 2a. Daily mean neutron ambient equivalent dose rate (μSv/h) measured by Rem-Counter is shown from 1st to 28th February 2013.

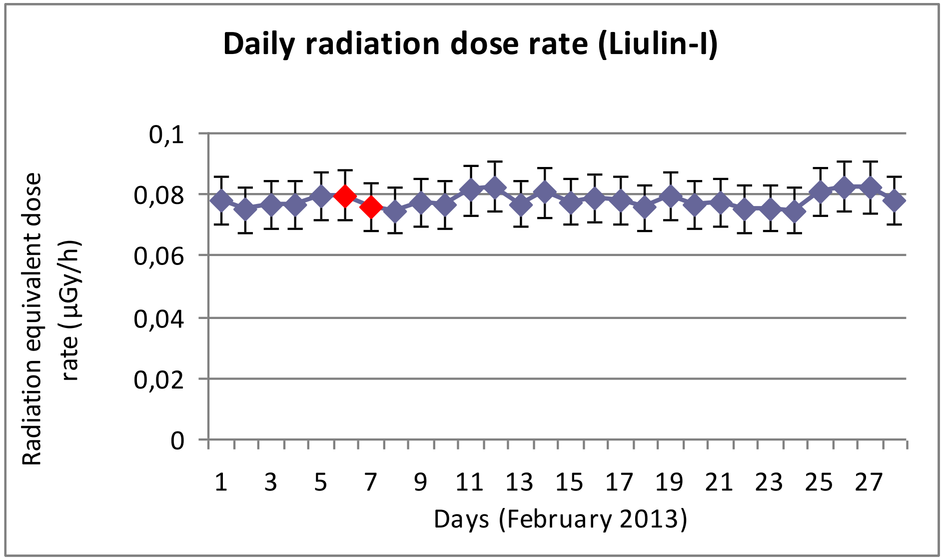

Liulin -Low LET - e.m,

Fig. 2b. Daily mean radiation equivalent dose rates (μGy/h) measured by Liulin-I is shown from 1st to 28th February 2013

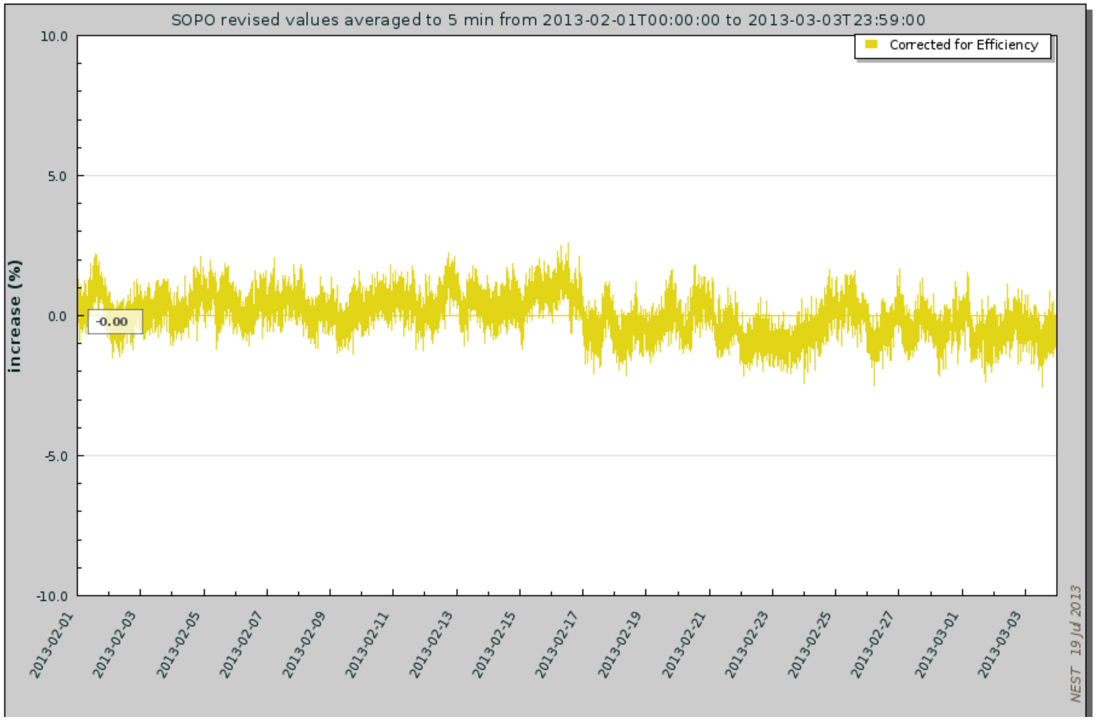

Neutron Monitor Database SOPO station

(http://www.nmdb.eu/nest/)

Assessment of cosmic events on NOAA / Space Weather Prediction Center

06 February: A CME with an earth-directed component was subsequently observed in LASCO C3 imagery at 06/0042 UTC. Geomagnetic field activity was predominantly quiet with two periods of unsettled conditions (08/0600-0900 UTC and 08/1500-1800 UTC) prompted by the 08/0400 UTC arrival of the 06 Feb CME.

18-24 February: 15 C-class flares were observed throughout the week, 13 of which originated from Region 1678 (N11, L=069, class/area=Dkc/470 on 21 Feb). This region was numbered on 18 Feb and quickly evolved from a beta to a complex beta-gamma-delta type magnetic configuration.

By 20 Feb, it had grown to 12 times its original size and produced the largest flare of the week, a C8/Sf at 24/1111 UTC. Geomagnetic field activity was at quiet levels until mid-day on 22 Feb when major storm levels were observed at high latitudes and the planetary K-index reached unsettled levels.

March 2013 measurements

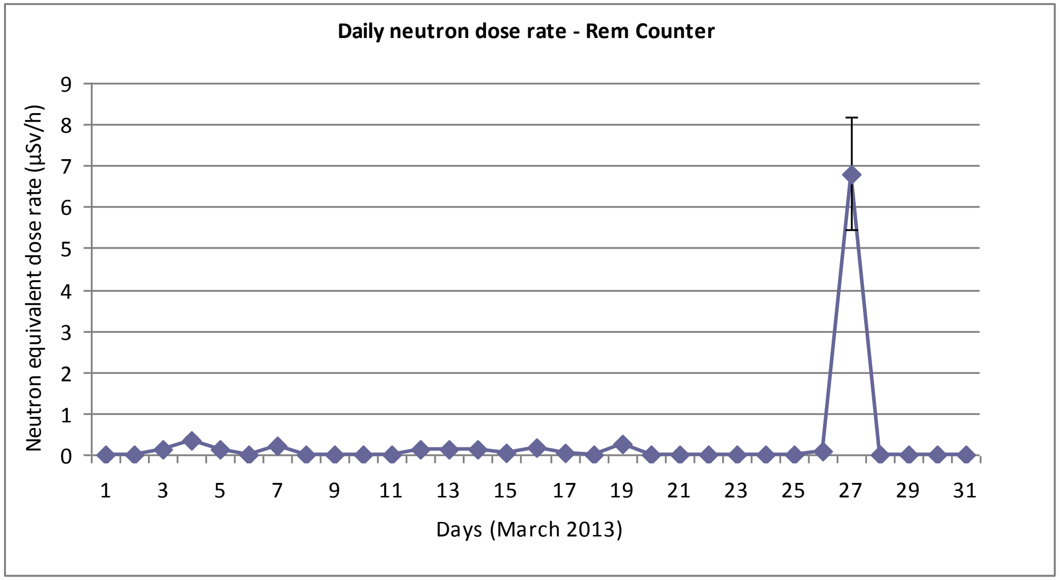

Rem Counter- Neutrons
-0.025 eV< En< 17 MeV

Fig. 3a. Daily mean neutron ambient equivalent dose rate (µSv/h) measured by Rem-Counter is shown for March 2013

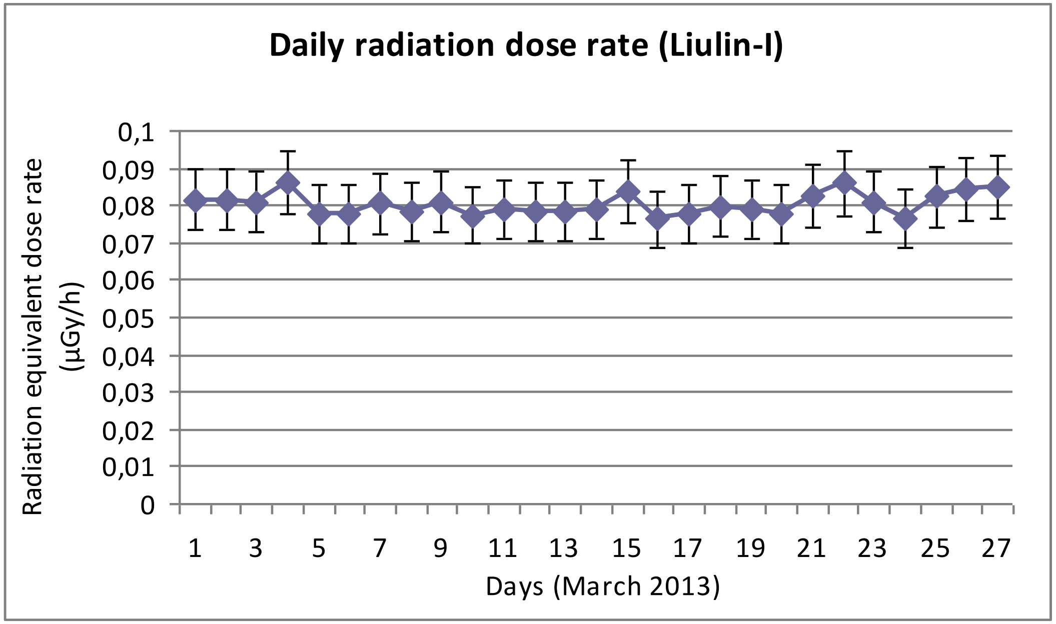

Liulin -Low LET - e.m,

Fig. 3b. Daily mean radiation equivalent dose rates (µGy/h) measured by Liulin-I is shown for March 2013.

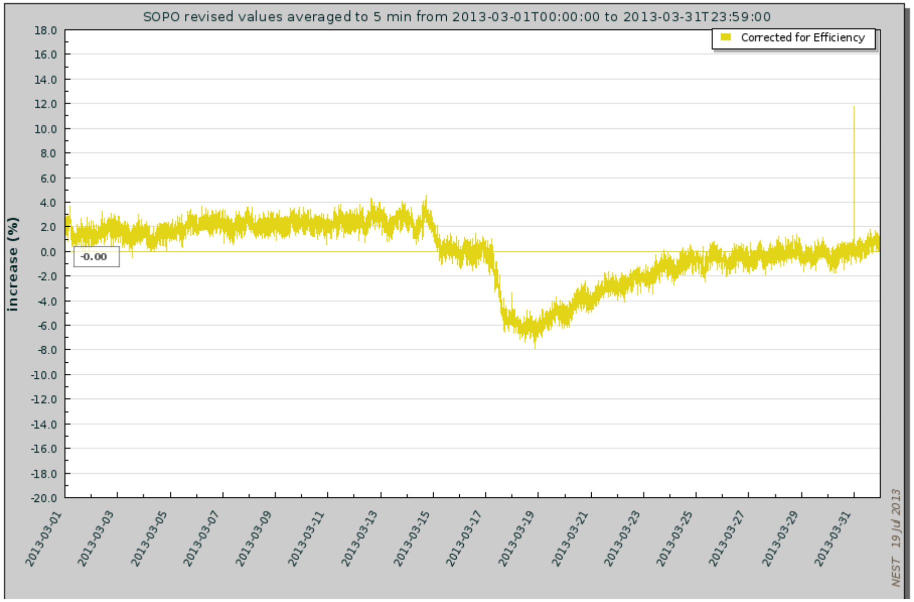

Neutron Monitor Database SOPO station (http://www.nmdb.eu/nest/)

Assessment of cosmic events on NOAA / Space Weather Prediction Center

12 March: A long duration C2/1f flare associated with a filament eruption near N20E05 occurred at around 12/1107 UTC. An associated asymmetric full halo was assessed to be Earth-directed with a velocity in the low 700 km/s range at departure.

Geomagnetic field activity increased slightly to yield a few isolated unsettled periods on 15-16 March due to weak effects from the 12 March CME.

15 March: Activity increased to moderate levels on 15 March when Region 1692 (N09, L=077, class/area Hhx/250 on 09 March) produced an M1/1f long duration flare at 15/0658 UTC. This flare appeared in H-alpha imagery to erupt along a NE to SW oriented filament channel and partially through Region 1692 beginning at 15/0615 UTC. Associated with this flare were a 150 sfu Tenflare, a Type IV radio sweep, and an asymmetrical full-halo CME (estimated plane-of-sky speed of 1399 km/s). The CME first appeared in SOHO/LASCO C2 imagery at 15/0712 UTC. Sudden Impulse (41 nT on the Boulder magnetometer) was observed as the 15 March CME became geoeffective.

21 March: Activity increased to moderate levels on 21 March when Region 1692 (N09, L=077, class/area Dki/340 on 20 Mar) produced an M1flare at 21/2204 UTC.

A filament eruption was observed around 19/1400 UTC from the area surrounding Region 1695 (N10, L=055, class/area Dao/180 on 18 Mar). A faint Earth-directed CME was associated with this event, as well as Type II (850 km/s) and Type IV radio sweeps.

April 2013 measurements

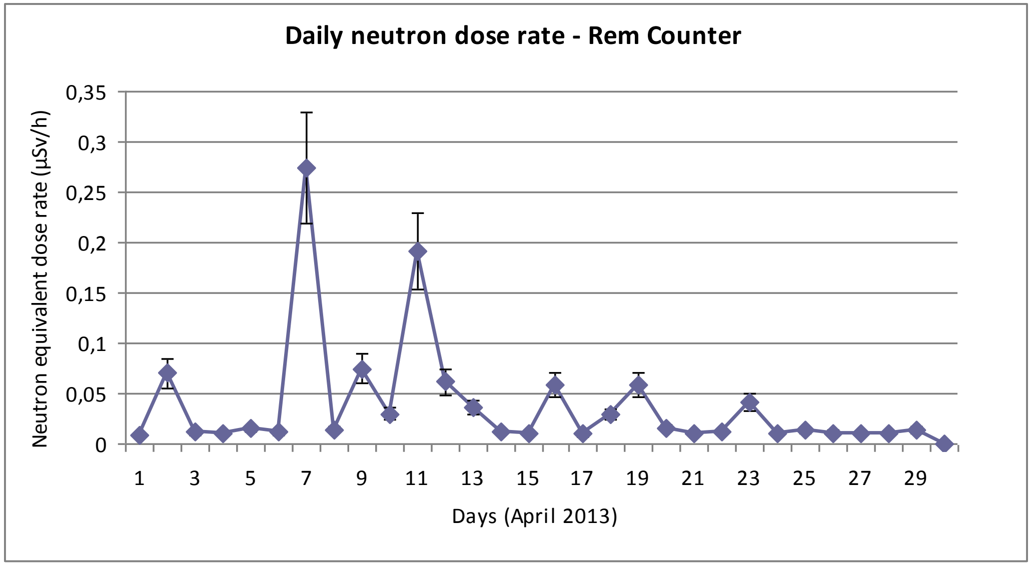

Rem Counter- Neutrons
-0.025 eV< En< 17 MeV

Fig. 4a. Daily mean neutron ambient equivalent dose rates (µSv/h) measured by Rem-Counter is shown for April 2013

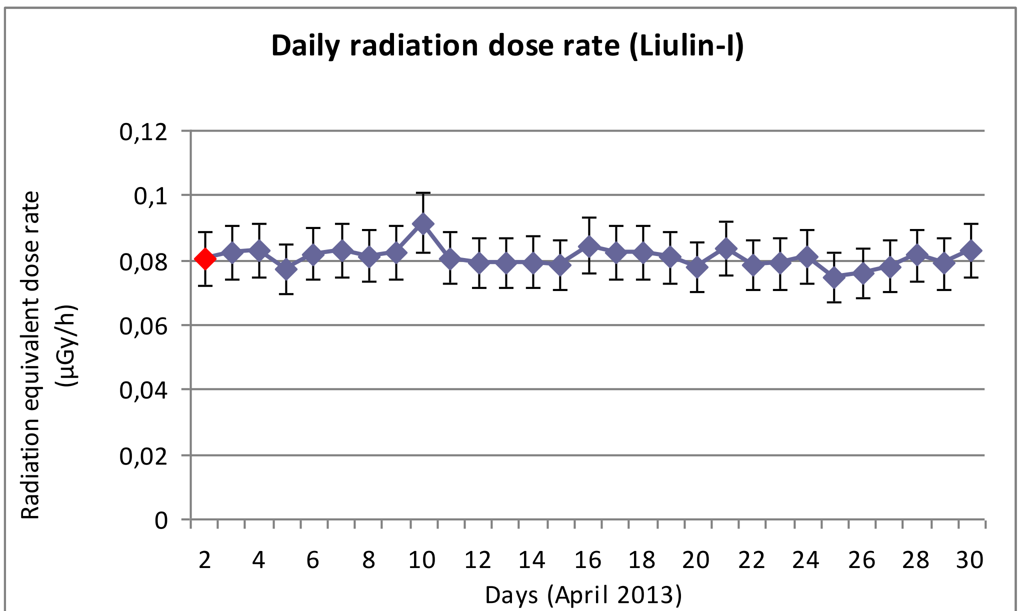

Liulin -Low LET - e.m,

Fig.4b . Daily mean radiation equivalent dose rate (µGy/h) measured by Liulin-I is shown for April 2013

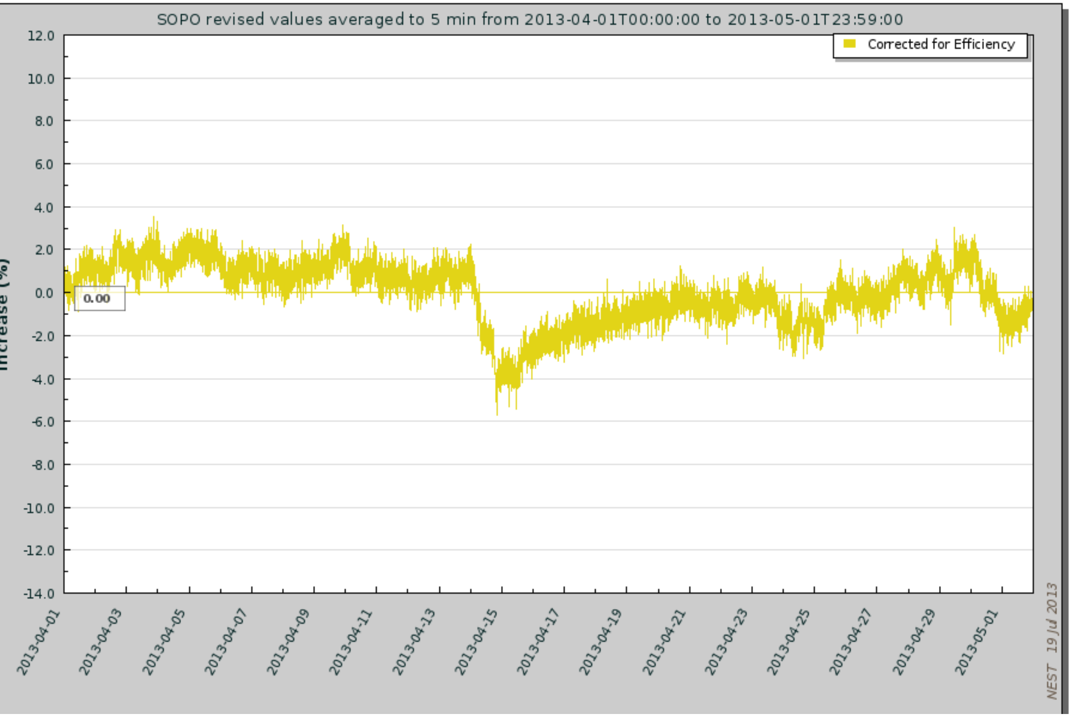

Neutron Monitor Database SOPO station

(http://www.nmdb.eu/nest/)

Assessment of cosmic events on NOAA / Space Weather Prediction Center

1-7 April: By 03 April, solar activity increased to low levels and continued at low levels through 04 April due to several low level C-class flares from Regions 1708 (N11, L=190, class/area Dao/090 on 29 March), 1711 (S19, L=158, class/area Cko/580 on 04 April), and 1713 (N10, L=175, class/area Dai/130 on 06 April).

By 05 April, solar activity reached moderate levels with an isolated M2 flare at 05/1748 UTC from Region 1719 (N08, L=076, class/area Dsi/150 on 07 April).Geomagnetic field activity was at quiet levels with isolated active periods at high latitudes mid-day on 01 and 07 April. Solar wind speed began the period decreasing from approximately 480 km/s to a low near 250 km/s by late on 05 April while the total field strength slowly increased from 2 nT to 6 nT. By Early on 06 April, solar wind speed started to increase to 340-370 km/s while total field strength increased to 5-7 nT.

30 April: *See May solar activity description.*

May 2013 measurements

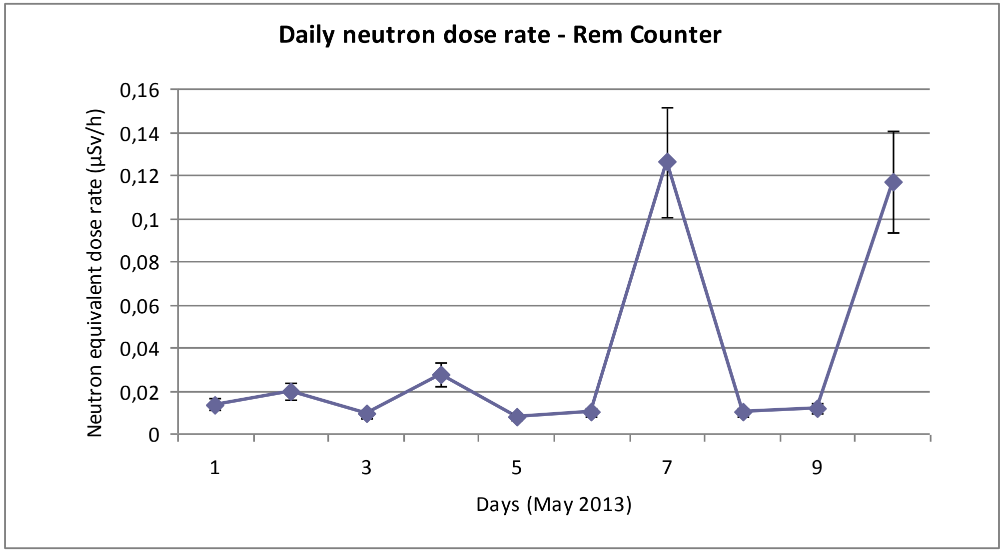

Rem Counter- Neutrons

-0.025 eV< En< 17 MeV

Fig. 5a. Daily mean neutron ambient equivalent dose rates (µSv/h) measured by Rem-Counter is shown from May 1st to May 10th 2013

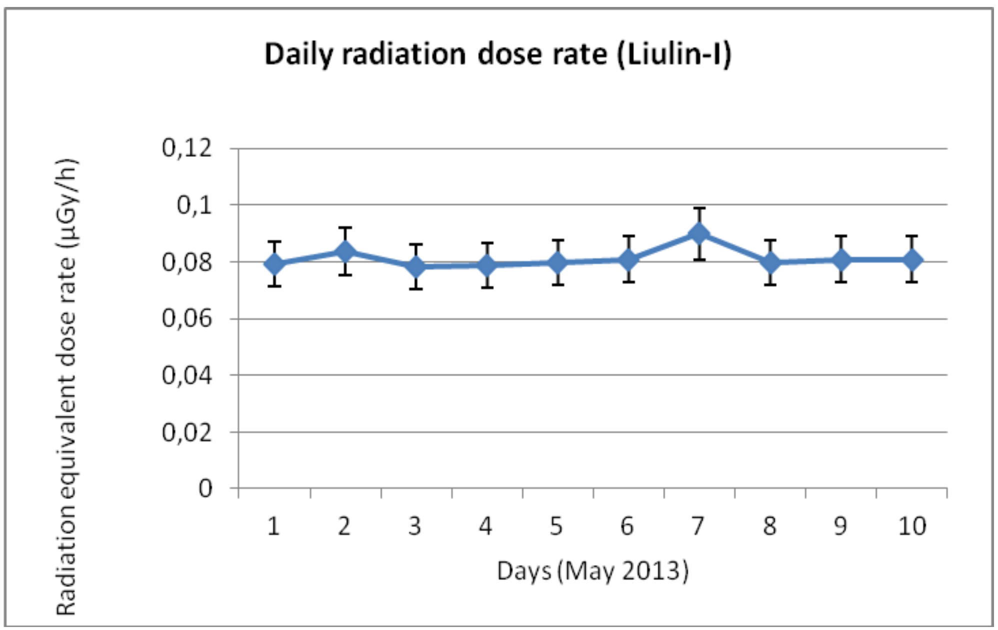

Liulin -Low LET - e.m,

Fig. 5c. Daily mean radiation equivalent dose rate (µGy/h) measured by Liulin-I is shown from My 1st to May 11th 2013

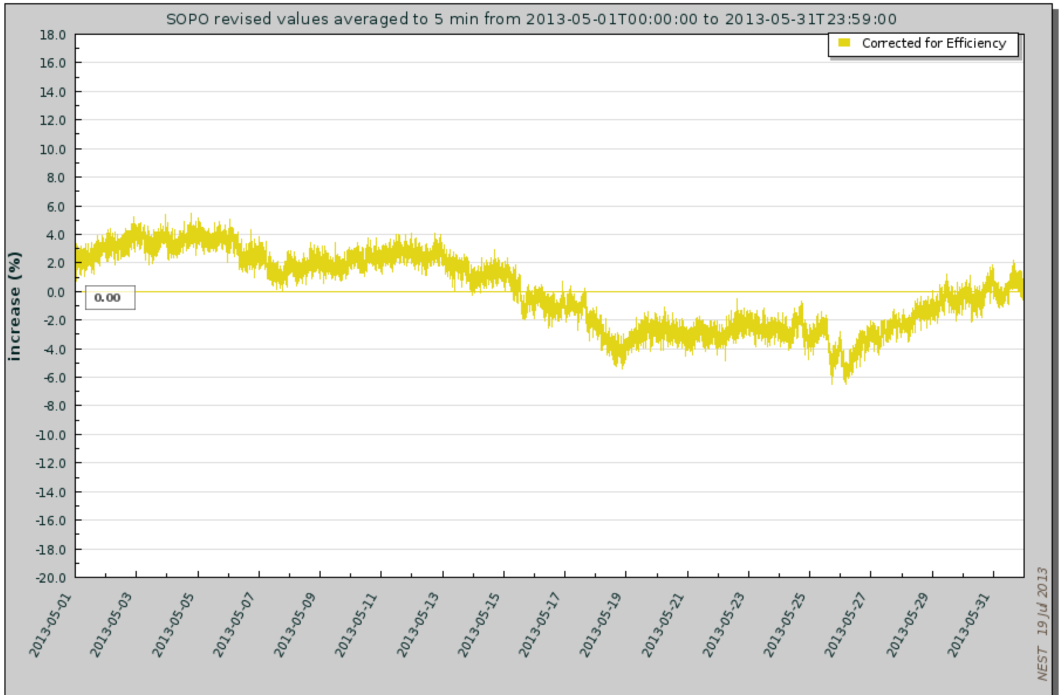

Neutron Monitor Database SOPO station

(http://www.nmdb.eu/nest/)

Assessment of cosmic events on NOAA / Space Weather Prediction Center

30 April - 2 May: The most prolific active region of the week was, by far, Region 1731 (N09, L=187, class/area=Dkc/420 on 28 Apr) with 17 C-class and two M-class flares to its credit. By 30 Apr, Region 1731 had developed beta-gamma-delta magnetic characteristics which it mainteined through 03 May.
During this period it produced an M1/1n flare at 02/0510Z and a long duration M1/2n flare at 03/1655Z. The 02 May event was associated with a tenflare (159 sfu), a Type II emission (703 km/s), and a CME first seen in LASCO/C2 imagery at 02/0524Z. The majority of the ejecta was directed north of the ecliptic, but output from the WSA-Enlil model suggested a possible scrape from the CME on **06 May**.
The **03 May** event was not associated with a CME.
Geomagnetic field activity reached ensettled to active levels beginning late on 30 Apr and lasting through 02 May. Conditions were quiet, with the exception of one unsettled period during the latter half of 05 May with the arrival of a corotating interaction region in advance of a positive polarity recurrent coronal hole high speed stream.

Radiation Measurements at Marambio Base (January-May 2013).

Month	(µE.m radiation Gy/h)	Neutrons (µSv/h)	TOTAL radiation (µSv/h)	% E.m radiation	% Neutrons
January	0,077	10,307 peaks (0,358) no peaks	0.436	17,75	82,26
February	0,078	0,121	0,199	39,15	60,85
March	0,080	0,283	0,363	22,09	77,91
April	0,081	0,039	0,120	67,38	32,62
May	0,082	0,035	0,117	69,86	30,14

Table 1. In the table are shown the monthly mean dose rate values recorded by Liulin-I (µGy/h) and Rem-Counter detectors (µSv/h), and the corresponding proportion of the total radiation.

Radiation	Energy	H* (µSv/h) mean values Jan-May		H*(mSv/year Annual dose
e.m and charged (LIULIN)	All energies	0,079		0,69
Neutrons (Rem Counter)	0.025 eV-17MeV	0,12		1,05
Neutrons (Bubbles)	0.025 eV-20 MeV	0,17		1,48
TOTAL				2.17 + -30%

Table 2. In the table are shown the monthly and yearly mean dose rate values recorded by Liulin-I (µGy/h) and Rem-Counter detectors (µSv/h), and the corresponding

Comparison with neutron Dose Equivalent at High Mountain observatories (0.025 eV<E_n <17 MeV)

The atmospheric neutron exposure (only considering the contribution of neutrons in the energy interval 0.025 eV-20 MeV) at Marambio base at sea level is comparable with the exposure in high mountain at lower latitudes.

Radiation	energy	H* (μSv/h) mean values January-March	Annual doseH* mSv/y
Liulin e.m and Charged	All energies	0.07	0.65
Rem counter Neutrons	0.025 eV-17 MeV	0.12	0.70
total		0.15	1.314

Marambio 64° 13'S – 56° 43'W	Chacaltaya 5230 m asl 16° 29' S- 68°8' W	Cervinia 3480 m asl 45°56' N - 07°42' E
0.12 (mSv/h)	0.09(μSv/h)	0.05(μSv/h)

The total ambient equivalent dose detected by rem counter (low energy neutron component) and Liulin (e.m. and charged component) is greater than 1 mSv.

Qualche dato…

Per ricevere una dose di 1 mSv

17 mesi a Parigi

6 mesi in luoghi a grande altitudine

7 voli andata e ritorno Parigi-Tokyo

13 voli andata e ritorno Parigi-New York sul Concorde

1 ½ giorni a bordo della MIR (400 km di altezza)

Per un dato volo, la dose totale della radiazione cosmica ricevuta è direttamente proporzionale alla durata dell'esposizione, e quindi alla durata del volo.

10 yr Career Exposure Limits - NCRP Report n. 132 (2000)

Age	Male (Sv)	Female (Sv)
25	0.7	0.4
35	1.0	0.6
45	1.5	0.9
55	3.0	1.7

Anatomical Location	NCRP Report n 132 (2000) (Gy-Eq) 1 year limit
Eye	2.0
Skin	3.0
BFO	0.50

NEUTRON DOSE EQUIVALENT RATE (ICRP 60) EVALUATED FROM UNFOLDED SPECTRA AT DIFFERENT ALTITUDES

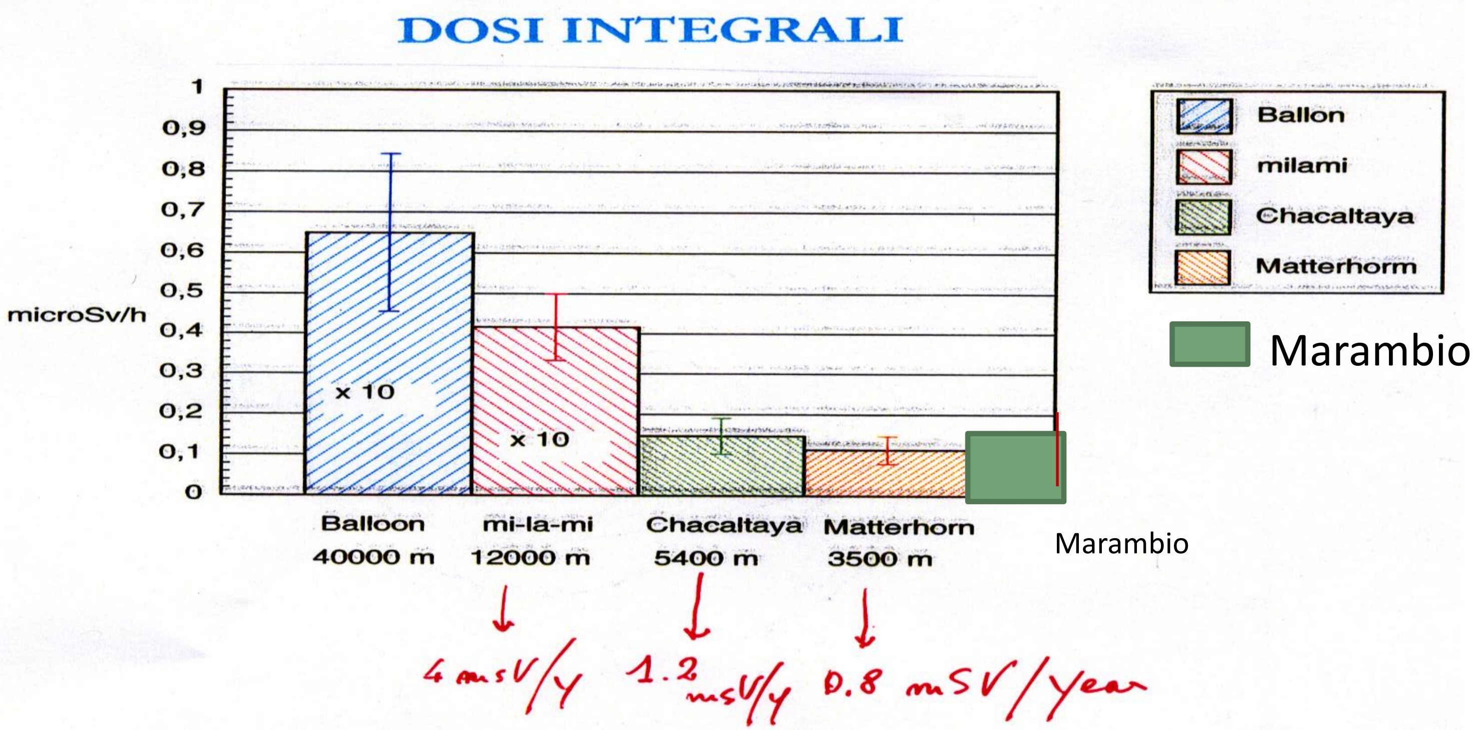

Allowed Limit of exposure H* (mSv) = 1 mSv/y

Professional exposure 5 mSv

Conclusions (1)

.

- In the first cosmic radiation campaign performed at Marambio base, preliminary results show evidence for an **environmental radiation intensity of about 1.4 mSv/year** considering the e.m and charged LowLET component (Liulin detector data) and the low energy (0.025 eV-20 MeV) neutron component (bubble detector and rem-counter data).

- In addition to this quantity, the high energy neutron component has to be considered, including the data obtained with the Bi209 stack (>200 MeV); these data will be available at the end of campaign, when the Bi209 stack will be analyzed..

- A considerable improvement in the neutron dose evaluation will be obtained whit the neutron energy spectrum knowledge, obtained by the unfolding of measurements of BDT, BDPND and Bi209, together with the use of appropriate ICRP74 Fluence to ambient dose equivalent neutron conversion factors.

- At present , it seems that the exposure at the cosmic radiation it is greater for people at high latitudes , (also considering the actual shift of magnetic South Pole location, -about 1800 km from the geographic South Pole). *As a consequence, a wide campaign is recommended in other austral location and at higher altitudes, for a better understanding of the influence of geographical position on the cosmic radiation exposure.*

-

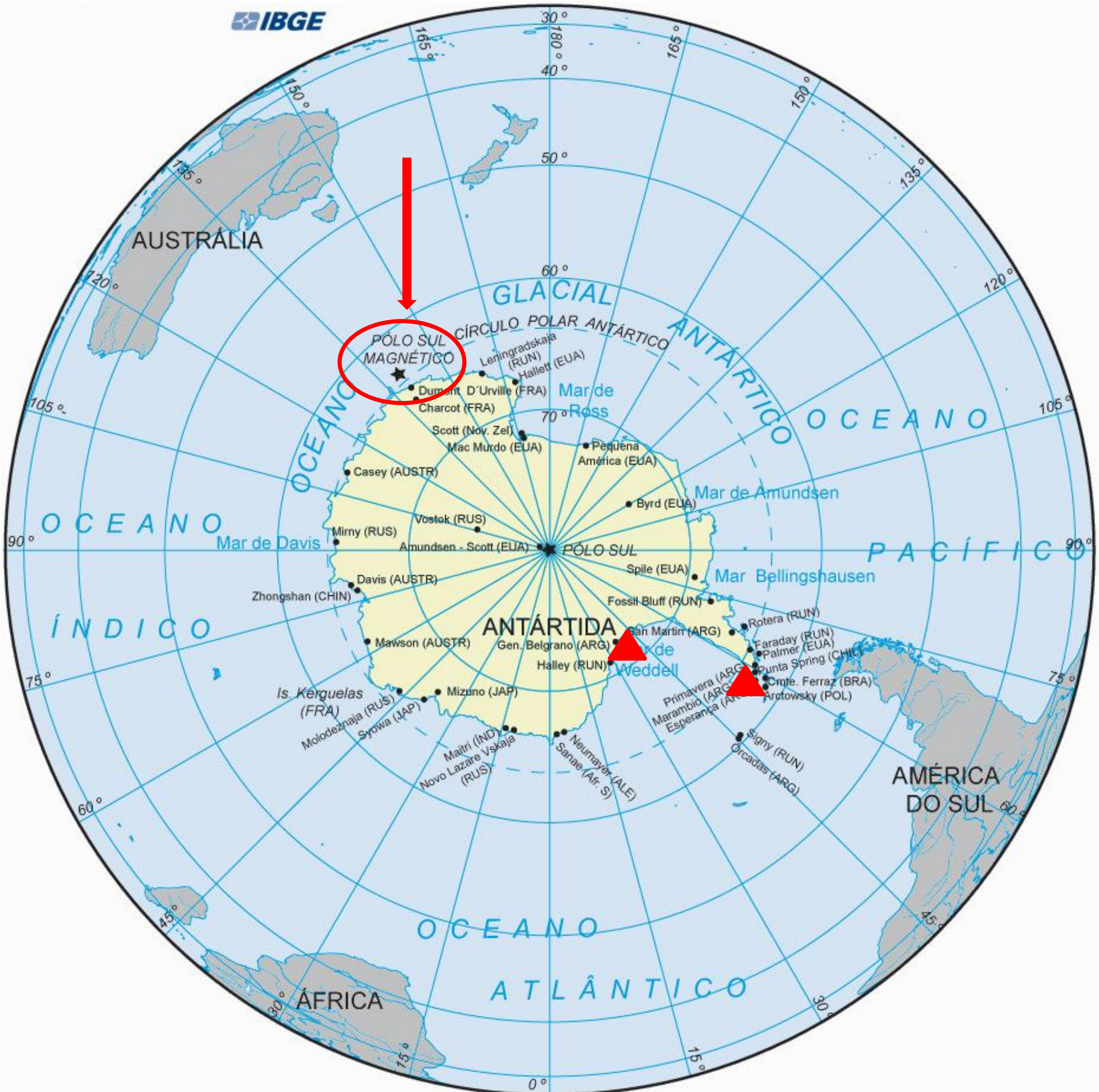
IBGE
AUSTRÁLIA
PÓLO SUL MAGNÉTICO
CÍRCULO POLAR ANTÁRTICO
GLACIAL
ANTÁRTICO
OCEANO
Mar de Ross
Mar de Amundsen
Mar Bellingshausen
OCEANO PACÍFICO
OCEANO ÍNDICO
Mar de Davis
ANTÁRTIDA
PÓLO SUL
Mar de Weddell
OCEANO ATLÂNTICO
AMÉRICA DO SUL
ÁFRICA
Is. Kerguelas (FRA)
Leningradskaja (RUN)
Hallett (EUA)
Dumont D'Urville (FRA)
Charcot (FRA)
Scott (Nov. Zel)
Mac Murdo (EUA)
Pequena América (EUA)
Casey (AUSTR)
Byrd (EUA)
Vostok (RUS)
Mirny (RUS)
Amundsen - Scott (EUA)
Spile (EUA)
Davis (AUSTR)
Zhongshan (CHIN)
Fossil Bluff (RUN)
San Martin (ARG)
Rotera (RUN)
Faraday (RUN)
Palmer (EUA)
Punta Spring (CHIL)
Cmte. Ferraz (BRA)
Arctowsky (POL)
Mawson (AUSTR)
Gen. Belgrano (ARG)
Halley (RUN)
Mizuno (JAP)
Molodeznaja (RUS)
Syowa (JAP)
Maitri (IND)
Novo Lazare Vskaja (RUS)
Neumayer (ALE)
Sanae (Afr. S)
Signy (RUN)
Orcadas (ARG)

Conclusions (2)

- Another interesting result, that requires further investigation, is the high intensity signal detected from the neutron rem counter in two occasions in January 2013, in which a sharp increasing of the neutron dose was evident; in this case the integral ambient equivalent dose reached 7 mSv, an amount dramatically greater than the allowed limit of 1 mSv/y.

- In both cases (8-10 January and 26-28 January) , solar flares directed to the earth were indicated by NOAA data. These phenomena have to be deeper investigated, together with the contemporary behavior of earth magnetic field.

- Other possibilities, as electromagnetic disturb due to radar or intense radio-signal seems to be excluded . In the future campaign it should be recommended to protect the instrumentation from any external disturb by a Faraday metallic shielding.

Future Work

On the base of the interesting results obtained in the 2013 campaign, a wide set of radiation measurements is planned , to better understand the radiation environment and the biological effects to the human being at high latitudes, also in correlation with solar activity

With this purpose new instrumentation will be used.

1 **The anthropomorphic phantom Jimmy**, to evaluate the neutron absorbed dose in critical organs and to obtain an indication of effective dose

2 **Two rem counter Snoopy (0.025 eV-17 eV)**

Linus 0.025 eV-400 MeV) with an extended response until to 400 MeV to separate the low energy and the high energy neutron components.

3 **BDS spectrometer** to evaluate in detail the neutron spectrum in 10 keV-20 MeV region

4 **Extended spectrometer** based on bubble detectors shielded with borate plastic and paraffine to better understand the intermediate energy region

5 **Gamma detector Na I** to evaluate the gamma radiation

6 **Two Liulin detectors** to evaluate the charged component

7 **GEANT4 Simulation**

8 Contemporary measurements at different latitudes and altitudes.

In this framework, it will be interesting to perform measurements both in Marambio and Belgrano Argentine base sand in Dome C Italian Base.

A project at PNRA have been submitted, to improve the scientific collaboration with La Plata University and the Istituto Antartico Argentino

Jimmy Phantom

The anthropomorphic phantom Jimmy has been designed and realized by INFN Sez. Torino, in collaboration with JRC Varese

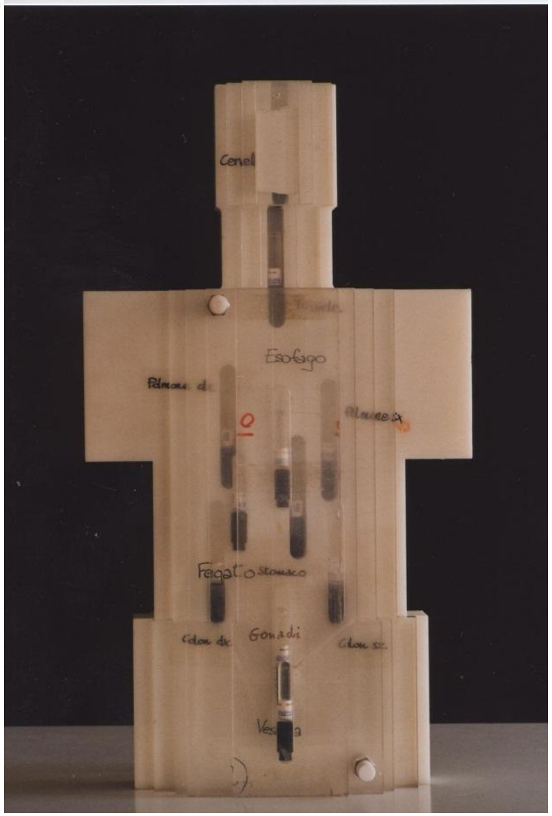

It consists of a phantom in polyethylene and plexiglas (tissue equivalent material), with inserted human bone in correspondence of column; composition follows the ICRP indications [1] .

Cavities are placed in correspondence of critical organs and are suitable to allocate passive dosemeters such as bubble detectors, TLDs, makrofolds.

This system allows to evaluate the neutron dose in depth

[1] ICRP -*Recommendation of the International Commission on Radiological Protection*, Pub. n.60, Oxford Pergamon (1991)

Jimmy Phantom

Advantages

- Cheap and easy-to-hand phantom
- Possibility to obtain an evaluation of the neutron dose in critical organs
- The holes can be used to contain different detectors (TLDs, bubble dosemeters, polycarbonate foils)
- It can be used for biological samples irradiations.

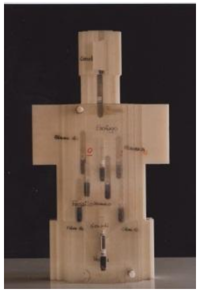

Applications

- Exposure under linear accelerators
- Calibration of personal dosemeters (JRC Second Standard Laboratory for calibration of personal dosemeters; Ispra, VA)
- Dosimetric measurements of cosmic ray neutron: intercontinental flights; high mountains Lab.; balloon flights.

Jimmy Phantom

Main physical characteristics:

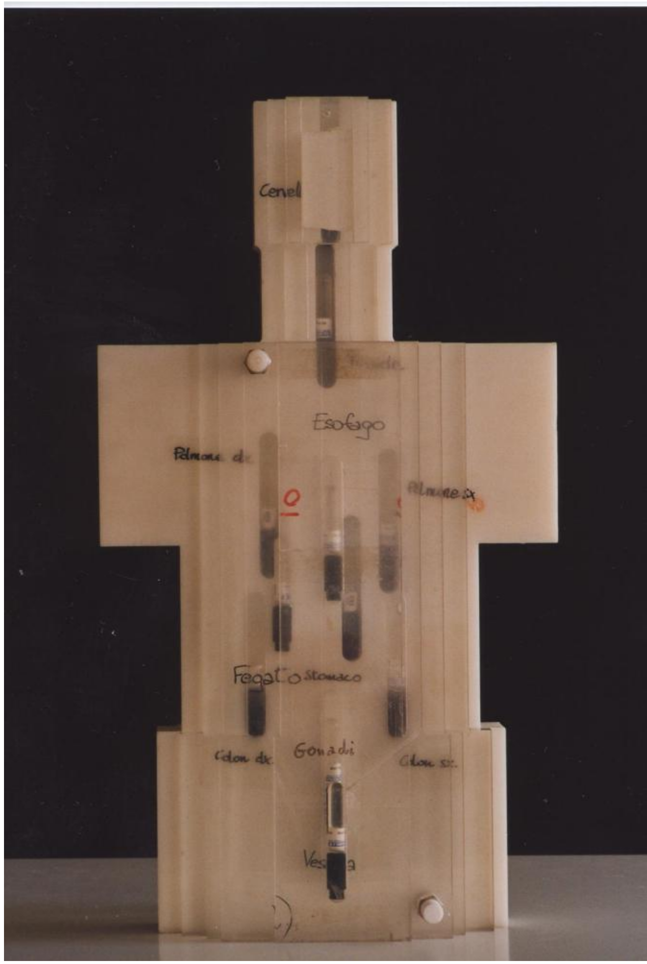

- Total weight: 37.1 kg
- 6 plexiglas slabs (21.6 kg)
  8% H, 32% C, 60% O
- 1 big polyethylene slab (14.2 kg)
  14.4% H, 85.6% C
- 1 human bone insert (1.2 kg)
  0.2% H, 41.4% O, 18.5% P, 39.9%Ca

  to simulate the spinal column
- Physical dimensions:

  head: 13.5x15x19 cm^3
  neck: 11x10x13.5 cm^3
  trunk: height 59 cm, max width 36 cm, thickness 20 cm

Future Work

The anthropomorphic phantom Jimmy, has been especially designed and constructed by INFN Torino, in collaboration with JRC Ispra (Varese,Italy) to evaluate the neutron absorbed dose in critical organs and to obtain an indication of Effective dose

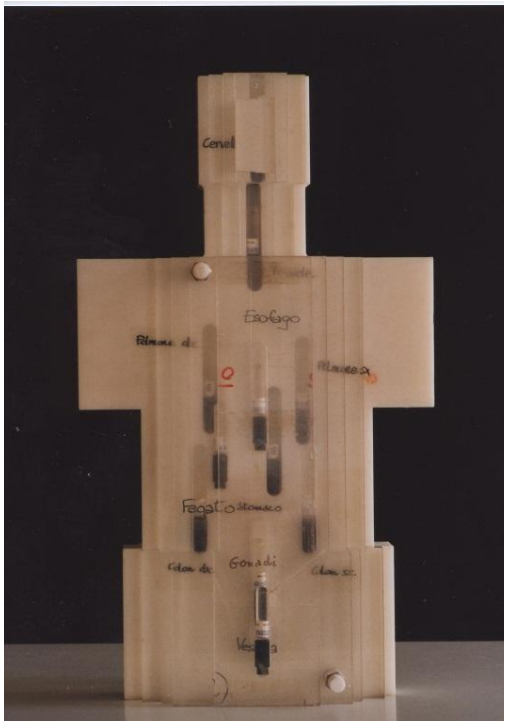

Jimmy Phantom

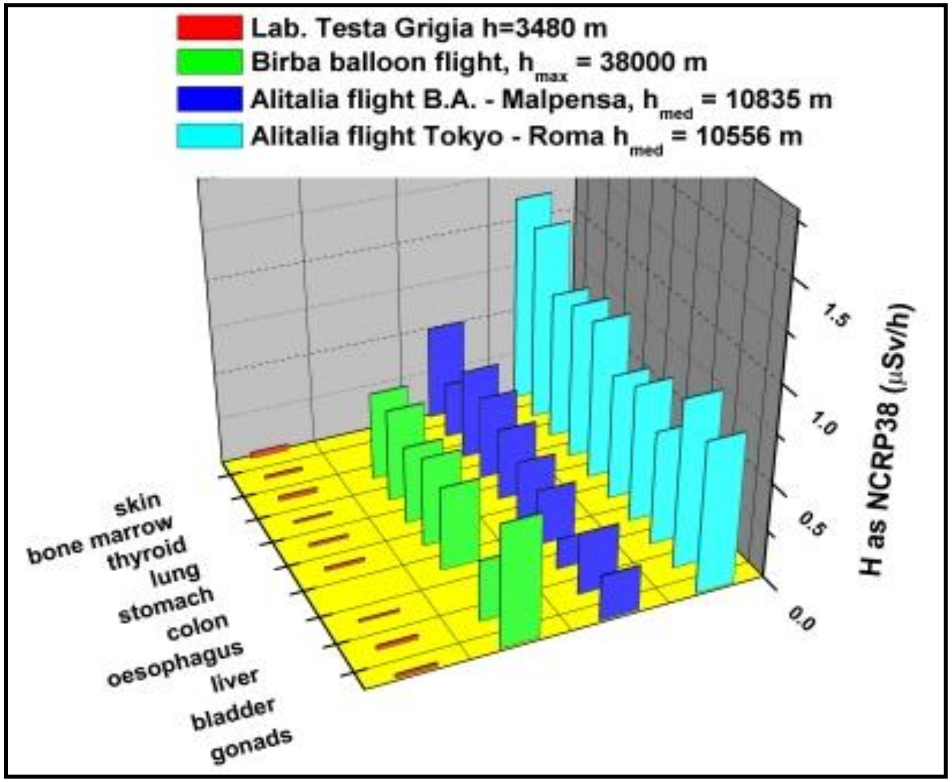

Neutron dose at critical organs measured by Jimmy Phantom in previous campaign at various altitudes

Marambio people

Arrival at the base

Researchers carrying the equipment

The Hercules of Fuerza Aerea Argentina

Thank you for your attention

Others experiments in Antarctic

CORA -Marambio

CORA Belgrano

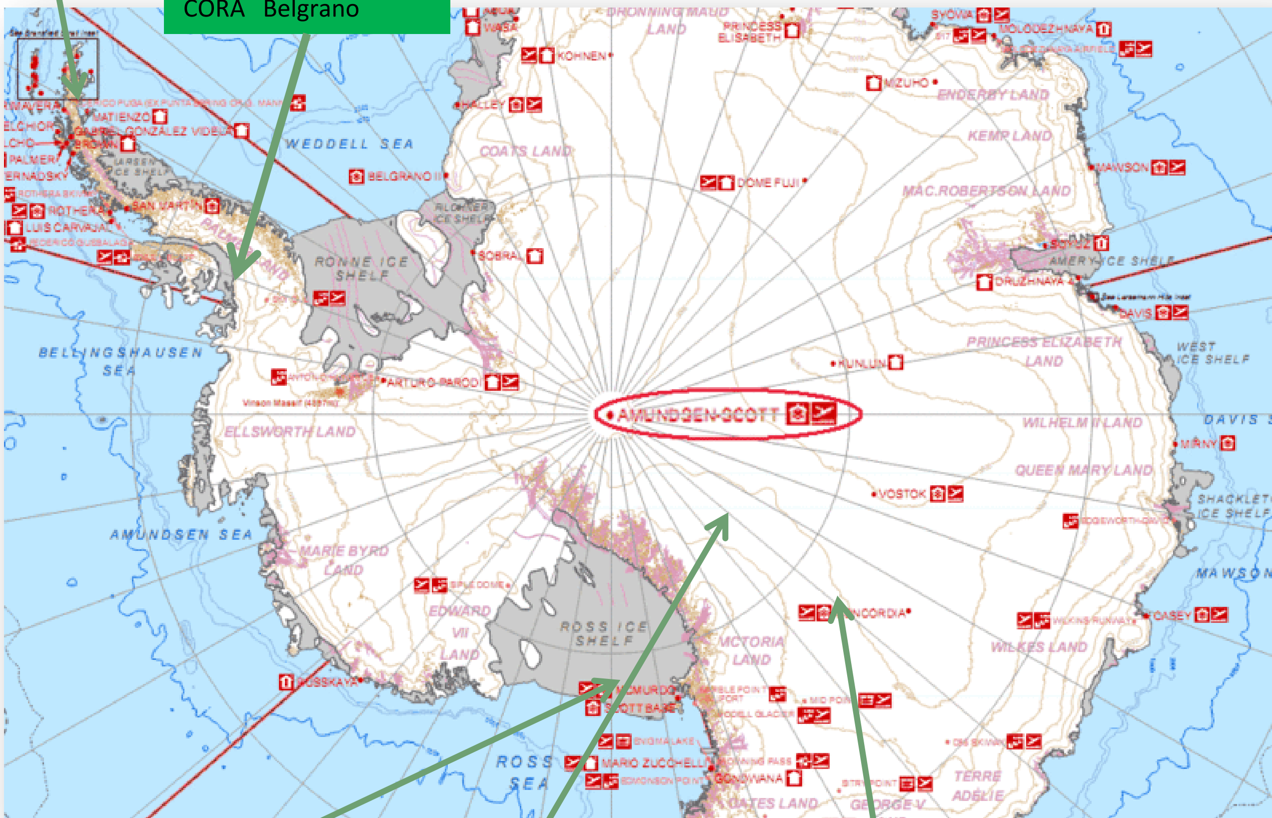

Boomerang-Mac Murdo

Ice Cube

Dome C

The inner Antarctic continent is the coldest and driest desert on Earth, offering an almost pristine nature without human contamination.

It is therefore a very appealing area to explore for the construction of astronomical facilities, but it offers also unique possibilities for others areas in scientific research, as astrophysics, paleoclimatology, extreme human physiology

Antarctic - Ice Cube

Search for neutrinos and strange particles at 1500 m deep

The detector dimension is 1 km3

A neutrino interaction with the electrons or nuclei of water can produce a charged particle that moves faster than the speed of light in the medium .This creates a cone of light -Cherenkov radiation- detected by optical sensors.

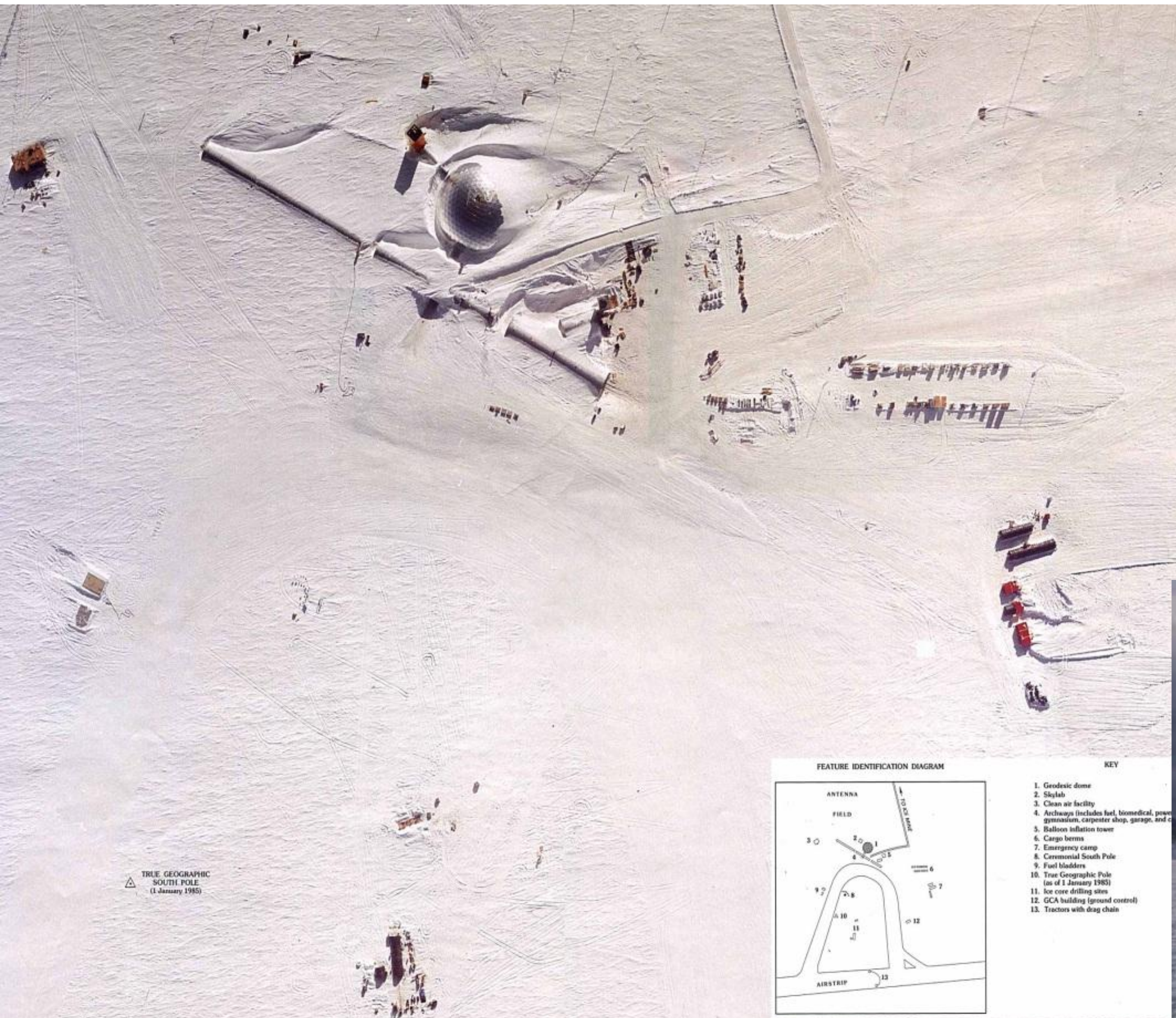

Hot water hose going at the hole in the ice

The ***IceCube Neutrino*** Observatory is a ***neutrino*** telescope at the Amundsen-Scott South Pole Station in Antarctica

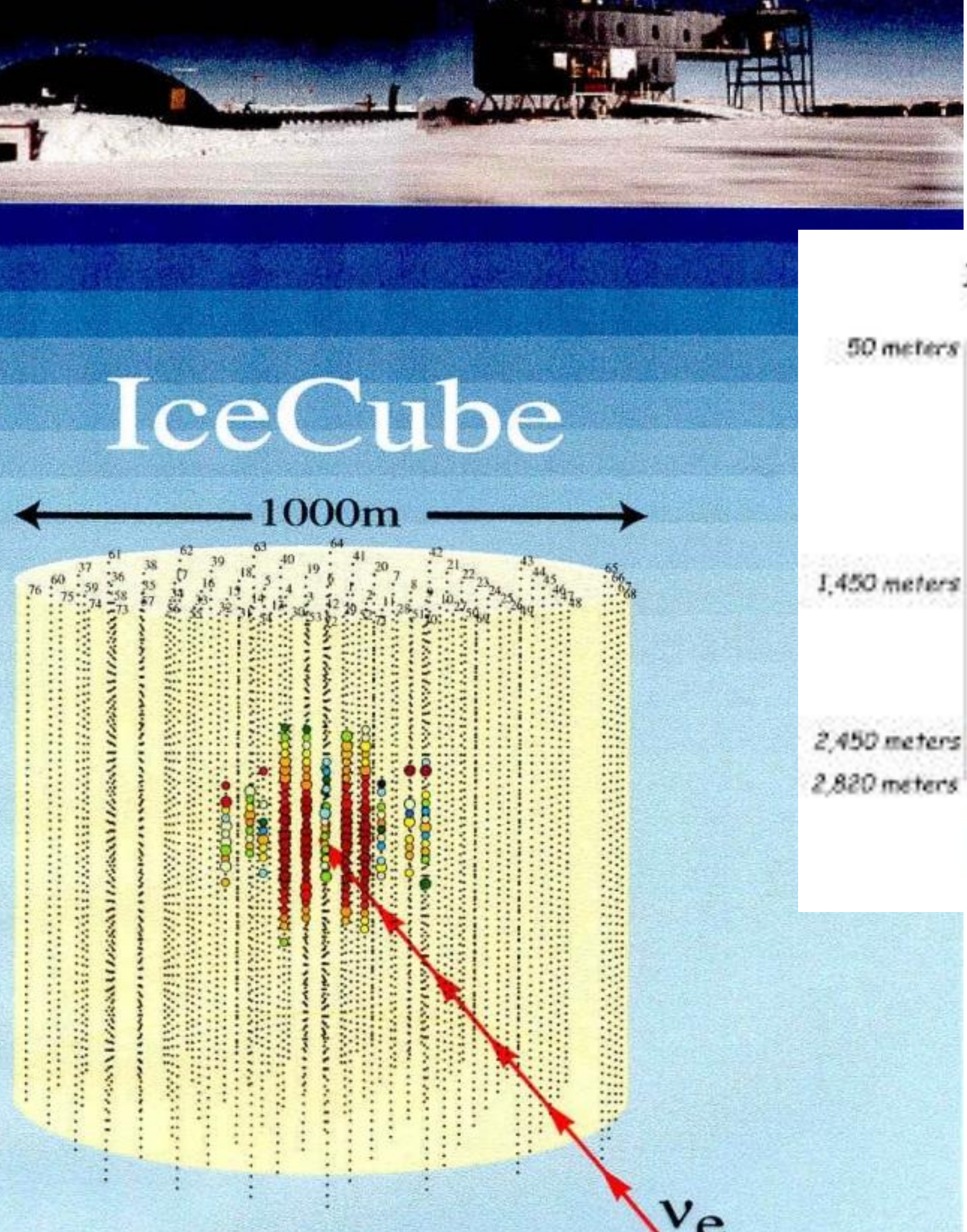

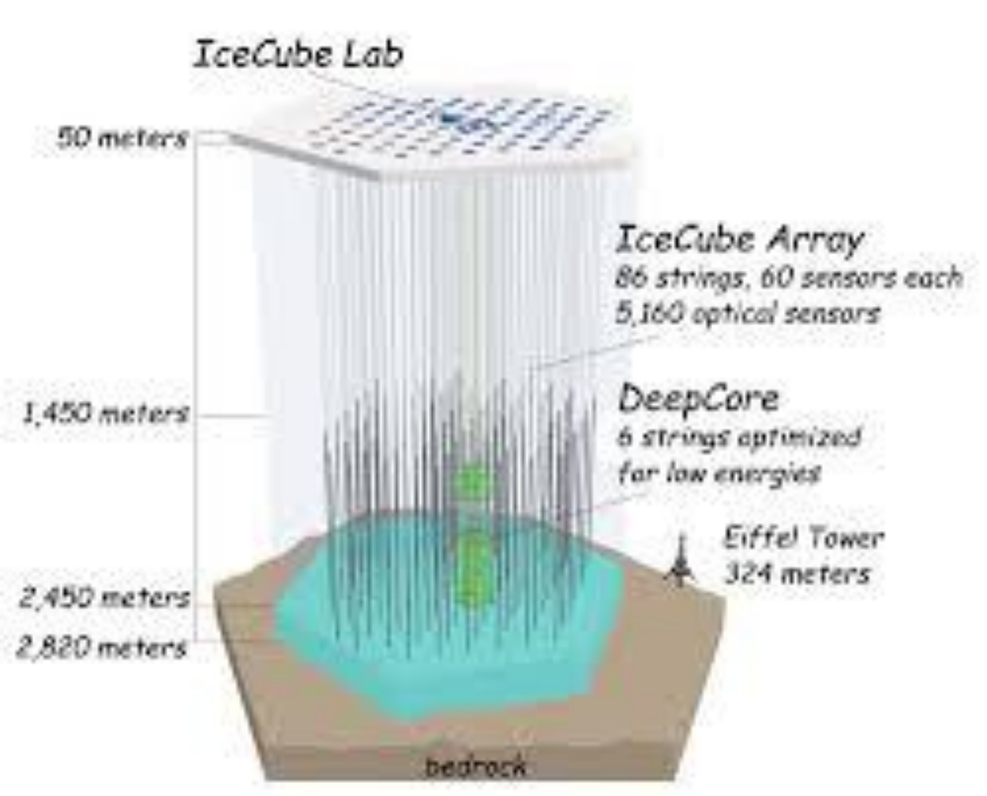

Science 22 November 2013:
Vol. 342 no. 6161

Evidence for High-Energy Extraterrestrial Neutrinos at the IceCube Detector

3 E12 eV – E15 eV

Study of Cosmic Microwave Background (CMB)

The gondola housing the BOOMERANG telescope.

The Boomerang experiment made the first map f the cosmic microwave background radiation (the First signal from the early universe, 480.000 years after the Big Bang. Trhee stratospheric balloon flight , carrying sofisticated radiotelescopes, were used. The instrument flew at 42 km altitude, transported by the anctarctic wind in a circle, returning at Mac Murdo base after two weeks

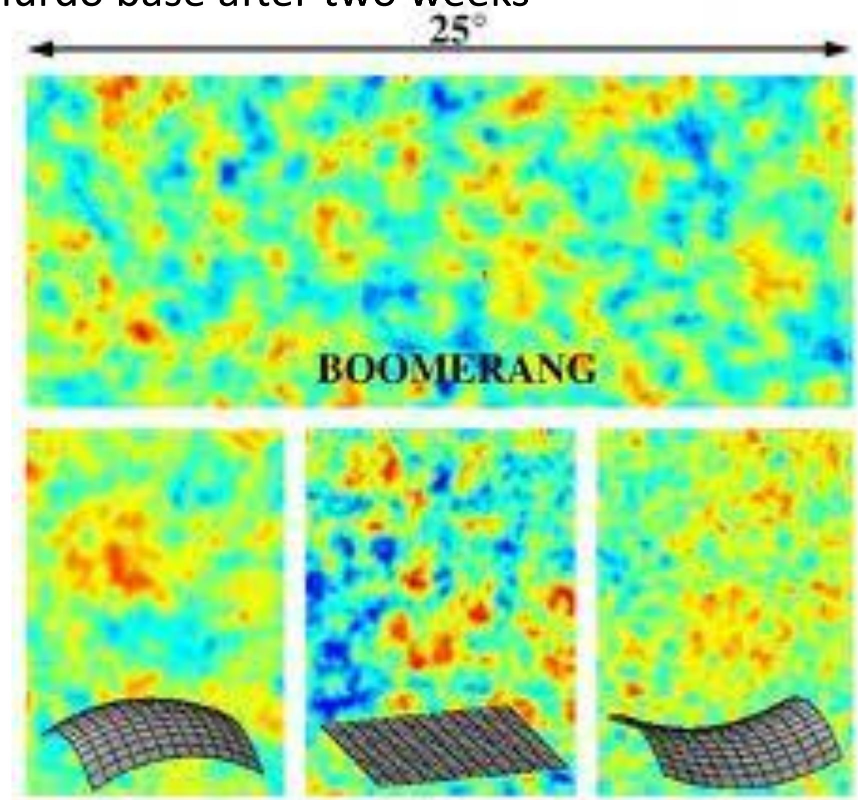

The BOOMERANG Telescope being readied for launch; in the background, Mount Erebus.

Concordia base is used as Human Exploration Analogue
for space experiments by ESA

Announcement of Opportunity
For Medical, Physiological and Psychological Research
Using Concordia Antarctic Station as Human Exploration
Analogue (AO-13-Concordia)

French-Italian Base Dome C Concordia.

BIOKIS - nDOSE

SHUTTLE STS134 MISSION 2011

Neutron detector set

- Bubble detector BDT thermal neutrons
- Bubble detector BD-PND fast neutrons
- Fission Bi209 stack relativistic neutrons


MF43C
BIOKIS 2 Container
BioS-SPORE
EU1 SPORULATION
BioS-SPORE
EU2 GERMINATION
VIDEO TAPES
FD 02
ENDEAVOUR
STS-134


Bio Kiss